

Quasinormal modes and emission rate of ModMax (A)dS black holes

Behzad Eslam Panah^{1,2,3} *, Angel Rincon⁴ †, Narges Heidari¹ ‡

¹ *Department of Theoretical Physics, Faculty of Science,*

University of Mazandaran, P. O. Box 47416-95447, Babolsar, Iran

² *ICRANet-Mazandaran, University of Mazandaran, P. O. Box 47416-95447 Babolsar, Iran*

³ *ICRANet, Piazza della Repubblica 10, I-65122 Pescara, Italy and*

⁴ *Departamento de Física Aplicada, Universidad de Alicante,*
Campus de San Vicente del Raspeig, E-03690 Alicante, Spain

By considering a new model of nonlinear electrodynamics, known as the modified Maxwell (ModMax), and taking into account the topological and the cosmological constants in Einstein's gravity, we extract black hole solutions called Topological ModMax (A)dS black holes. The next step is to study the thermodynamic properties, quasinormal modes, and emission rates of these black holes in order to examine the impact of ModMax's parameter and the cosmological constant on these systems. To achieve this, we obtain the quasinormal spectra for massless scalar, electromagnetic, and Dirac perturbations. Additionally, we calculate null geodesics and determine the radius of the critical orbit. We then apply this information to derive the angular velocity and the Lyapunov exponent, which represent the real and imaginary terms of the quasinormal modes in the eikonal limit, respectively. Furthermore, we investigate the energy emission rate based on the discussion of null geodesics and the shadow radius.

I. INTRODUCTION

The nonlinear electrodynamics (NED) theories were introduced to address some of the problems in Maxwell's theory, such as the singularity that occurs at the position of a point-like charge. This singularity is one of the main issues in Maxwell's theory. One of the most well-known NED theories is the Born-Infeld (BI) theory [1]. The BI theory arises as the effective action in an open super-string theory and D-brains. It has a non-singular self-energy of the point-like charge (see Refs. [2, 3] for more details). However, the BI-NED theory is less symmetric than Maxwell's theory. Although this NED theory possesses a fundamental $SO(2)$ duality [4], it features a dimensionful parameter and, therefore, is no longer conformally invariant. On the other hand, Maxwell's theory is the only theory with two fundamental symmetries: electromagnetic duality and conformal invariance. Recently, a new model of NED was introduced in Refs. [5, 6], which includes the same symmetries as Maxwell's theory. This NED theory is known as the Modification of Maxwell (ModMax) theory. The ModMax theory is characterized by a dimensionless parameter γ (ModMax parameter) and reduces to Maxwell's theory when $\gamma = 0$ (see Refs. [7–33] for more details on the ModMax theory).

Bekenstein and Hawking discovered an analogy between the geometric properties of black holes and thermodynamic variables that provides a profound understanding of the relationship between the physical properties of gravity and classical thermodynamics [34]. The thermodynamic properties of black holes, particularly phase transition and thermal stability, are of great importance as they offer insights into the underlying structure of spacetime geometry. Phase transition also plays a significant role in various fields such as elementary particles [35], usual thermodynamics [36], condensed matter [37], black holes [38], and cosmology [39]. Another intriguing aspect of black hole thermodynamics is the phase transition in anti-de Sitter (AdS) spacetime, which is motivated by AdS/CFT duality [40]), and provides valuable insights into the quantum nature of gravity. The study of phase transition in AdS black holes within an extended phase space has gained considerable attention in recent years. In this perspective, the cosmological constant can be considered as a variable, identified as thermodynamic pressure [41], while the black hole's mass is interpreted as enthalpy [42].

Isolated black holes are ideal objects and are considered starting points for studying a more realistic situation. Black holes are never isolated, so they interact with their surroundings and perturb the background. After such an interaction, the black hole responds by emitting gravitational waves, which are parameterized by (quasinormal) modes with characteristic frequencies. Such modes have a non-vanishing imaginary part, and they contain all the information about how the black holes relax after the perturbation. It should be emphasized that the quasinormal

* email address: eslampanah@umz.ac.ir

† email address: angel.rincon@ua.es

‡ email address: heidari.n@gmail.com

frequencies are affected by i) the geometry itself, and ii) the type of perturbation "applied" to the background (scalar, vector, tensor, or fermionic), and they are independent of the initial conditions.

During the ring-down phase of a black hole merger, a unique perturbed object is created. This is when the geometry of spacetime undergoes damped oscillations due to the emission of gravitational waves. In this context, quasi-normal modes (QNMs) play a significant role. To understand the underlying physics of gravitational waves, black hole perturbation theory is essential. Several references such as [43–48] provide valuable insights in this field, while more recent work, in which a wide variety of methods and a wide range of backgrounds have been investigated, can be found in [49–77] and references therein. Gravitational wave astronomy provides a powerful tool for testing gravity under extreme conditions. While there is a vast amount of literature available, some excellent reviews on the subject can be found at [78–80]. Additionally, Chandrasekhar's seminal monograph [81] delves into non-trivial details, covering the canonical aspects of black hole physics.

The study of QNMs is relevant not only for their constraints on the parameters of the black hole but also for their connection with area quantization. Therefore, it is now more important than ever to investigate the QN spectrum of black holes, which is precisely one of the main goals of this manuscript.

On the other hand, a method of analytically evaluating the QNMs in the geometric-optics (eikonal) limit has been introduced in Ref. [82]. Furthermore, Ref. [83] demonstrates that in this eikonal limit, QNMs are associated with the properties of a null particle situated on the unstable circular geodesic of the spacetime. This relationship has been confirmed in the majority of static, spherically symmetric, asymptotically flat spacetimes. The real part of the QNM is interpreted as the angular velocity at the unstable null geodesic, while the imaginary part is connected to the Lyapunov exponent, corresponding to the instability time scale of the orbit [84–88].

After a brief and concise introduction, we proceed to introduce and summarize the relevant equations within the framework of ModMax theory and topological black hole solutions. Moving on to section III, we delve into the investigation of black hole thermodynamics, including the calculation of thermal stability. Section IV is dedicated to the computation of the corresponding QNMs for i) scalar, ii) electromagnetic, and iii) Dirac perturbations. The analysis of QNMs in eikonal limits is presented in section V. Subsequently, in section VI, we delve into the discussion of the energy emission rate for various parameters of the ModMax black hole. Finally, we conclude and discuss our findings in the last section.

II. MODMAX THEORY AND TOPOLOGICAL BLACK HOLE SOLUTIONS

The action describing the coupling of Einstein's gravity with the ModMax electrodynamics and the cosmological constant is expressed as

$$\mathcal{I} = \frac{1}{16\pi} \int_{\partial\mathcal{M}} d^4x \sqrt{-g} [R - 2\Lambda - 4\mathcal{L}], \quad (1)$$

where R and Λ are, respectively, the Ricci scalar and the cosmological constant. The determinant of the metric tensor $g_{\mu\nu}$ is defined as $g = \det(g_{\mu\nu})$. In the above action, \mathcal{L} refers to ModMax's Lagrangian and is given [5, 6]

$$\mathcal{L} = \mathcal{S} \cosh \gamma - \sqrt{\mathcal{S}^2 + \mathcal{P}^2} \sinh \gamma, \quad (2)$$

where γ is referred to as ModMax's parameter, which is a dimensionless quantity. Additionally, \mathcal{S} and \mathcal{P} represent a true scalar and a pseudoscalar, respectively, in the following expressions

$$\mathcal{S} = \frac{\mathcal{F}}{4}, \quad (3)$$

$$\mathcal{P} = \frac{\tilde{\mathcal{F}}}{4}, \quad (4)$$

in the equations above, the term $\mathcal{F} = F_{\mu\nu}F^{\mu\nu}$ is referred to as the Maxwell invariant. Moreover, $F_{\mu\nu}$ represents the electromagnetic tensor field and is defined as $F_{\mu\nu} = \partial_\mu A_\nu - \partial_\nu A_\mu$, with A_μ being the gauge potential. Additionally, $\tilde{\mathcal{F}} = F_{\mu\nu}\tilde{F}^{\mu\nu}$, where $\tilde{F}^{\mu\nu} = \frac{1}{2}\epsilon^{\mu\nu\rho\lambda}F_{\rho\lambda}$. It is worth noting that the Lagrangian of ModMax (Eq. (2)) reduces to the Maxwell theory (i.e., $\mathcal{L} = \frac{\mathcal{F}}{4}$) when $\gamma = 0$.

In this work, we are interested in studying electrically charged black holes within the framework of Einstein's theory, taking into account the presence of the cosmological constant. Therefore, we can set $\mathcal{P} = 0$ in the Lagrangian of ModMax (Eq.(2)).

The generalized Einstein-ModMax's equations in the presence of the cosmological constant write in the following form [7]

$$G_{\mu\nu} + \Lambda g_{\mu\nu} = 8\pi T_{\mu\nu}, \quad (5)$$

$$\partial_\mu \left(\sqrt{-g} \tilde{E}^{\mu\nu} \right) = 0, \quad (6)$$

where $T_{\mu\nu}$ is the energy-momentum tensor which is given by

$$8\pi T^{\mu\nu} = 2 \left(F^{\mu\sigma} F^\nu{}_\sigma e^{-\gamma} \right) - 2e^{-\gamma} \mathcal{S} g^{\mu\nu}, \quad (7)$$

and $\tilde{E}_{\mu\nu}$ is defined as

$$\tilde{E}_{\mu\nu} = \frac{\partial \mathcal{L}}{\partial F^{\mu\nu}} = 2 \left(\mathcal{L}_S F_{\mu\nu} \right), \quad (8)$$

where $\mathcal{L}_S = \frac{\partial \mathcal{L}}{\partial \mathcal{S}}$.

For charged case, the ModMax field equation (Eq. (6)), turns to

$$\partial_\mu \left(\sqrt{-g} e^{-\gamma} F^{\mu\nu} \right) = 0. \quad (9)$$

Notably, by setting $\gamma \neq 0$ a birefringence phenomenon occurs [5]; apart from the lightlike polarization mode there exists another mode which is subluminal for $\gamma > 0$ and superluminal for $\gamma < 0$, hinting on a physical restriction $\gamma \geq 0$.

Here, we consider a four-dimensional static metric in the following form

$$ds^2 = -f(r) dt^2 + \frac{dr^2}{f(r)} + r^2 d\Omega_k^2, \quad (10)$$

where $f(r)$ is the metric function in which we must find it. In addition, $d\Omega_k^2$ is given by

$$d\Omega_k^2 = \begin{cases} d\theta^2 + \sin^2 \theta d\varphi^2 & k = 1 \\ d\theta^2 + d\varphi^2 & k = 0 \\ d\theta^2 + \sinh^2 \theta d\varphi^2 & k = -1 \end{cases}. \quad (11)$$

To have a radial electric field, we use the following gauge potential

$$A_\mu = h(r) \delta_\mu^t, \quad (12)$$

and by applying the metric (10) and the MaxMax field equation (9), we can get

$$2h'(r) + rh''(r) = 0, \quad (13)$$

where the prime and double prime are, respectively, the first and second derivatives with respect to r . We can solve the above equation which leads to

$$h(r) = -\frac{q}{r}, \quad (14)$$

where q is an integration constant related to the electric charge.

In order to get the metric function, $f(r)$, we apply the equations (5), (7), (10), and (14). After some calculation, we can obtain the following differential equations

$$eq_{tt} = eq_{rr} = rf'(r) + f(r) + \Lambda r^2 - k + \frac{q^2}{r^2} e^{-\gamma} = 0, \quad (15)$$

$$eq_{\theta\theta} = eq_{\varphi\varphi} = f''(r) + \frac{2}{r} f'(r) + 2\Lambda - \frac{2q^2}{r^4} e^{-\gamma} = 0, \quad (16)$$

which eq_{tt} , eq_{rr} , $eq_{\theta\theta}$, and $eq_{\varphi\varphi}$ are representative tt , rr , $\theta\theta$, and $\varphi\varphi$ components of Eq. (5), respectively. Using the differential equations (15) and (16), we extract the metric function in the following form

$$f(r) = k - \frac{m}{r} - \frac{\Lambda r^2}{3} + \frac{q^2 e^{-\gamma}}{r^2}, \quad (17)$$

where m is an integration constant that is related to the geometrical mass of the black hole. It is notable that the obtained metric function (17) satisfies all the components of the field equation (5), simultaneously. Moreover, the metric function Eq. (17) turns to topological Reissner-Nordstrom (A)dS black hole when $\gamma = 0$, i.e.

$$f(r) = k - \frac{m}{r} - \frac{\Lambda r^2}{3} + \frac{q^2}{r^2}. \quad (18)$$

To find the singularity of the obtained solutions (17), we calculate the Kretschmann scalar. For this aim, by considering the metric (10) and the metric function (17), we can obtain the Kretschmann scalar in the following form

$$R_{\alpha\beta\gamma\delta}R^{\alpha\beta\gamma\delta} = \frac{8\Lambda^2}{3} + \frac{12m^2}{r^6} - \frac{48mq^2e^{-\gamma}}{r^7} + \frac{56q^4e^{-2\gamma}}{r^8}, \quad (19)$$

which indicates that the Kretschmann scalar diverges at $r = 0$ (i.e., $\lim_{r \rightarrow 0} R_{\alpha\beta\gamma\delta}R^{\alpha\beta\gamma\delta} \rightarrow \infty$). Therefore, there is a curvature singularity located at $r = 0$. Also, it is finite for $r \neq 0$. The asymptotic behavior of spacetime is determined by $\lim_{r \rightarrow \infty} R_{\alpha\beta\gamma\delta}R^{\alpha\beta\gamma\delta} \rightarrow \frac{8\Lambda^2}{3}$, and $\lim_{r \rightarrow \infty} f(r) \rightarrow -\frac{\Lambda r^2}{3}$, where shows the spacetime will be asymptotically de Sitter (dS) or anti de Sitter (AdS), for $\Lambda > 0$ (or $\Lambda < 0$).

Here, we want to study the effect of the ModMax's parameter and topological constant k on the obtained metric function (17). For this purpose, we plot $f(r)$ versus r in Figs. 1–4. Our findings are:

i) For $\Lambda < 0$ two roots can be found, one of which is related to the inner horizon and the other to the event horizon. It is noteworthy that the number of roots decreases from two to one when γ is increased (see left panels in Figs. 1–4). As one can see in the left panel of Fig. 1, the large black holes belong to the negative value of the topological constant, i.e. $k = -1$.

ii) For $\Lambda > 0$ we can have three, two, and one root(s), see the right panels in Figs. 1–4. Our results in the left panel of Fig. 1 show that for $k = 0, k = -1$, there is no event horizon. However, for $k = +1$, there may be three roots comprising an inner horizon (the small root), an event horizon (the middle root), and a cosmological horizon (the largest root), see the right panels in Figs. 1 and 2. In addition, by increasing γ , the number of roots also changes.

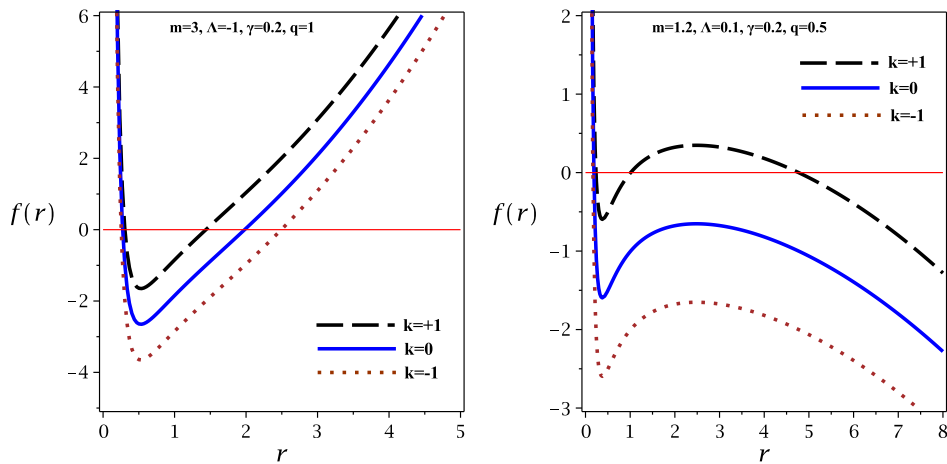


FIG. 1: The metric function $f(r)$ versus r for different values of the topological constant (k). Left panel for AdS case ($\Lambda < 0$). Right panel for dS case ($\Lambda > 0$).

III. CONSERVED AND THERMODYNAMIC QUANTITIES: THE FIRST LAW OF THERMODYNAMICS

To investigate the thermodynamic properties of these black holes, we first obtain the Hawking temperature of the black holes. For this purpose, we express the geometrical mass (m) in terms of the radius of the event horizon (r_+), the cosmological constant (Λ) and the electrical charge (q), the ModMax parameter (γ) and the topological constant (k). We therefore solve $g_{tt} = f(r) = 0$, which leads to the following result

$$m = kr_+ - \frac{\Lambda r_+^3}{3} + \frac{q^2 e^{-\gamma}}{r_+}. \quad (20)$$

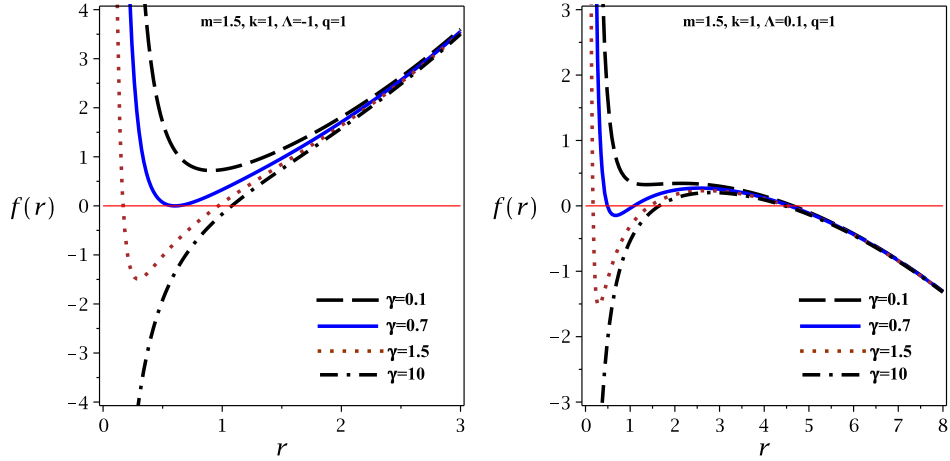


FIG. 2: The metric function $f(r)$ versus r for $k = +1$, and different values of the ModMax's parameter. Left panel for AdS case ($\Lambda < 0$). Right panel for dS case ($\Lambda > 0$)

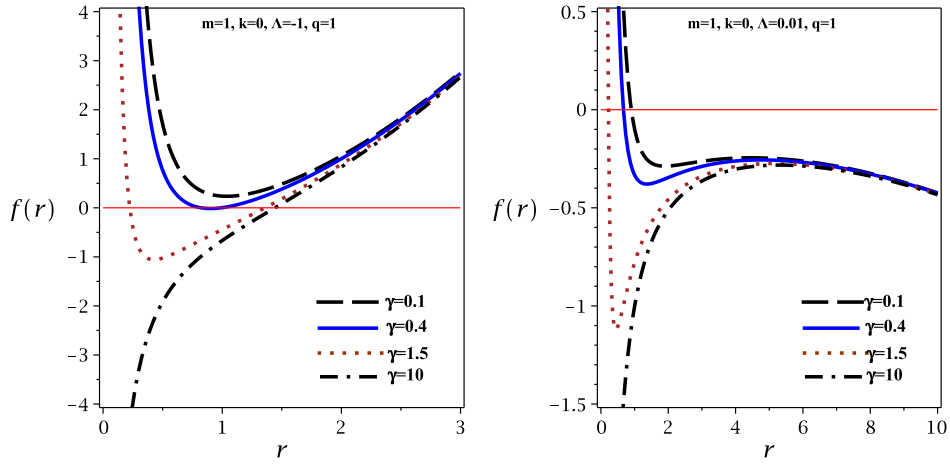


FIG. 3: The metric function $f(r)$ versus r for $k = 0$, and different values of the ModMax's parameter. Left panel for AdS case ($\Lambda < 0$). Right panel for dS case ($\Lambda > 0$).

The Hawking temperature is defined as

$$T_H = \frac{\kappa}{2\pi}, \quad (21)$$

where κ is related to the surface gravity by

$$\kappa = \sqrt{\frac{-1}{2} (\nabla_\mu \chi_\nu) (\nabla^\mu \chi^\nu)}. \quad (22)$$

By using the metric (10), the Killing vector $\chi = \partial_t$, and Eq. (22), we can extract the surface gravity which leads to

$$\kappa = \frac{1}{2} \left. \frac{\partial f(r)}{\partial r} \right|_{r=r_+}, \quad (23)$$

so, by applying Eqs. (20)-(23), we can get the Hawking temperature in the following form

$$T_H = \frac{1}{4\pi} \left(\frac{k}{r_+} - \Lambda r_+ - \frac{q^2 e^{-\gamma}}{r_+^3} \right), \quad (24)$$

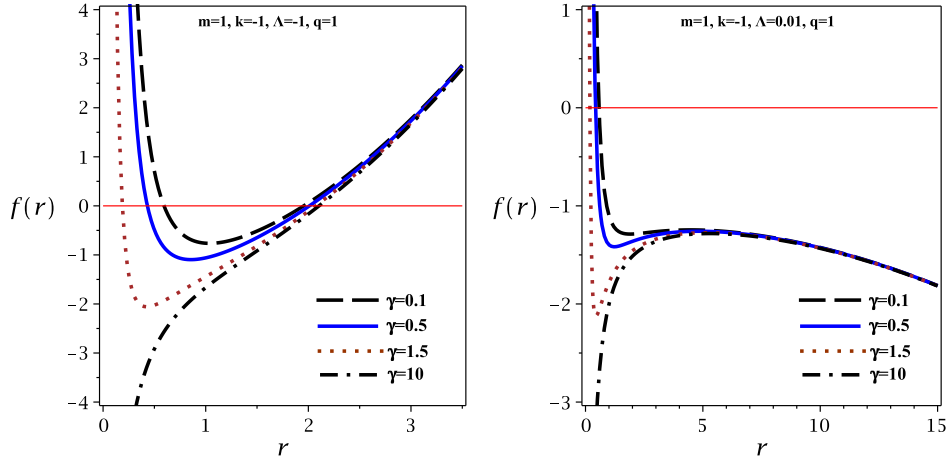


FIG. 4: The metric function $f(r)$ versus r for $k = -1$, and different values of the ModMax's parameters. Left panel for AdS case ($\Lambda < 0$). Right panel for dS case ($\Lambda > 0$).

where it depends on the cosmological constant (Λ), electrical charge (q), the ModMax's parameter (γ), and topological constant (k). Furthermore, the Hawking temperature of small black holes (or in high energy limit of the Hawking temperature) depends on the ModMax's parameter and electrical charge, i.e.

$$\lim_{r_+ \rightarrow 0} T \propto -\frac{q^2 e^{-\gamma}}{4\pi r_+^3}, \quad (25)$$

but for large black holes (or the asymptotic limit of the Hawking temperature) it only depends on the cosmological constant as

$$\lim_{r_+ \rightarrow 0} T \propto -\frac{\Lambda r_+}{4\pi}. \quad (26)$$

Using the Gauss law, we can extract the electric charge of black hole per unit volume (\mathcal{V}), in the following form

$$Q = \frac{\tilde{Q}}{\mathcal{V}} = \frac{F_{tr}}{4\pi} \int_0^{2\pi} \int_0^\pi \sqrt{g_k} d\theta d\varphi = \frac{q}{4\pi}. \quad (27)$$

where $F_{tr} = \frac{q}{r^2}$, and for case $t = \text{constant}$ and $r = \text{constant}$, the determinant of metric tensor g_k is $r^4 \det(d\Omega_k^2)$ (i.e., $g_k = \det(g_k) = r^4 \det(d\Omega_k^2)$). Furthermore, $\mathcal{V} = \int_0^{2\pi} \int_0^\pi \sqrt{\det(d\Omega_k^2)} d\theta d\varphi$, where is the area of a unit volume of constant (t, r) space. For example, \mathcal{V} is 4π for $k = 1$.

The electric potential at the event horizon (U) with respect to the reference ($r \rightarrow \infty$) is obtained as

$$U = A_\mu \chi^\mu |_{r \rightarrow \infty} - A_\mu \chi^\mu |_{r \rightarrow r_+} = \frac{q e^{-\gamma}}{r_+}, \quad (28)$$

where the gauge potential is zero when $r \rightarrow \infty$.

Applying the area law, we can get the entropy of the topological ModMax black holes per unit volume (\mathcal{V}), which leads to

$$S = \frac{\tilde{S}}{\mathcal{V}} = \frac{\mathcal{A}}{4\mathcal{V}} = \frac{\int_0^{2\pi} \int_0^\pi \sqrt{g_{\theta\theta} g_{\varphi\varphi}} |_{r=r_+}}{4} = \frac{r_+^2}{4}, \quad (29)$$

where \mathcal{A} is the horizon area.

Using Ashtekar-Magnon-Das (AMD) approach [89, 90], we can get the total mass of the topological ModMax black holes per unit volume (\mathcal{V}), which is

$$M = \frac{\tilde{M}}{\mathcal{V}} = \frac{m}{8\pi} = \frac{1}{8\pi} \left(k r_+ - \frac{\Lambda r_+^3}{3} + \frac{q^2 e^{-\gamma}}{r_+} \right), \quad (30)$$

in the above equation, we use from the geometrical mass (20).

Now, we are in a position to indicate that the obtained conserved and thermodynamics quantities in Eqs. (24), (27), (28), (29), and (30), satisfy the first law of thermodynamics in the following form

$$dM = TdS + UdQ, \quad (31)$$

where $T = \left(\frac{\partial M}{\partial S}\right)_Q$, and $U = \left(\frac{\partial M}{\partial Q}\right)_S$ are, respectively, in agreement with those of calculated in Eqs. (24) and (28).

IV. QUASINORMAL MODES

As already mentioned, the QNMs represent the characteristic frequencies at which the scalar field oscillates and the rate at which it is damped. The QNMs provide a crucial insight into the ModMax parameter's influence on the scalar field's behavior and its impact on the effective potential. In order to determine the corresponding QNMs, we need to solve a Schrodinger-like equation while satisfying certain boundary conditions. These conditions include the requirement for purely incident waves at the event horizon and purely outgoing waves at infinity. Due to the inherent complexity of the differential equation, it is often not possible to find an exact analytical solution. Analytical solutions for QNMs are only possible under certain conditions. To overcome this challenge, we rely on a variety of semi-analytical and numerical methods to obtain the aforementioned frequencies. For potential barriers that exhibit well-behaved characteristics, the semi-analytical approach of WKB is a valuable method for finding QNMs.

A. Spin zero case (scalar field)

The corresponding wave equation of a massless minimally coupled scalar field Φ is described by the Klein-Gordon equation, namely [91–93]

$$\frac{1}{\sqrt{-g}}\partial_\mu\left(\sqrt{-g}g^{\mu\nu}\partial_\nu\right)\Phi = 0. \quad (32)$$

To progress and obtain the QNMs, it is convenient to apply the method of separation of variables, which is the conventional approach, i.e.

$$\Phi(t, r, \theta, \phi) = e^{-i\omega t} \frac{\psi(r)}{r} Y_\ell^m(\theta, \phi), \quad (33)$$

where Y_ℓ^m are the spherical harmonics and ω is the QN frequency to be determined. Thus, by applying the above ansatz, we can decouple the differential equation to obtain an ordinary differential equation for the radial part only, which is a Schrödinger-like equation of the following form

$$\frac{d^2\psi}{dx^2} + [\omega^2 - V(x)]\psi = 0, \quad (34)$$

in which x is the so-called tortoise coordinate, defined using the following expression

$$x \equiv \int \frac{dr}{f(r)}. \quad (35)$$

In addition, the effective potential barrier can be found with the help of the following expression

$$V_s(r) = f(r) \left(\frac{\ell(\ell+1)}{r^2} + \frac{f'(r)}{r} \right), \quad \ell \geq 0 \quad (36)$$

where the prime represents differentiation with respect to r , and ℓ is the angular degree. In particular, for the lapse function given in Eq. (17), the effective potential takes the simple form

$$V_s(r) = \left(k - \frac{m}{r} + \frac{q^2 e^{-\gamma}}{r^2} - \frac{\Lambda r^2}{3} \right) \left[\frac{\ell(\ell+1)}{r^2} + \frac{1}{r} \left(\frac{m}{r^2} - \frac{2q^2 e^{-\gamma}}{r^3} - \frac{2\Lambda r}{3} \right) \right]. \quad (37)$$

At this point, some comments are in order. First, from the left column of Figure (5) we observe the effect of the ModMax parameter γ on the effective potential for different values of the angular number ℓ for scalar perturbations.

TABLE I: QN frequencies for scalar perturbations, setting $k = 1$, $m = 2$, $\Lambda = 0.1$, $q = 1$ for several different values of the ModMax parameter γ and varying ℓ . For comparison reasons, we also show the frequencies of the classical geometry, i.e., when $\gamma = 0$. It should be noted that as the ModMax parameter increases, the quasinormal frequencies decrease. Thus, the ModMax parameter has a screening effect on the QNMs.

γ	n	$\ell = 6$		$\ell = 7$		$\ell = 8$		$\ell = 9$		$\ell = 10$	
0.0	0	1.105370	-0.0602992 i	1.276770	-0.0603201 i	1.44803	-0.0603337 i	1.61919	-0.0603429 i	1.79028	-0.0603498 i
0.0	1	1.103310	-0.1809210 i	1.274790	-0.1810040 i	1.44623	-0.1810430 i	1.61762	-0.1810580 i	1.78886	-0.1810740 i
0.0	2	1.100060	-0.3013760 i	1.270920	-0.3018030 i	1.44245	-0.3019130 i	1.61444	-0.3018660 i	1.78598	-0.3018750 i
0.0	3	1.098260	-0.4204130 i	1.265350	-0.4227110 i	1.43618	-0.4232270 i	1.60960	-0.4228450 i	1.78158	-0.4228250 i
0.2	0	0.928142	-0.0593617 i	1.072230	-0.0593736 i	1.21618	-0.0593814 i	1.36002	-0.0593870 i	1.50380	-0.0593911 i
0.2	1	0.926750	-0.1781290 i	1.071010	-0.1781560 i	1.21512	-0.1781690 i	1.35907	-0.1781820 i	1.50294	-0.1781900 i
0.2	2	0.923966	-0.2970300 i	1.068550	-0.2970520 i	1.21305	-0.2970210 i	1.35716	-0.2970400 i	1.50122	-0.2970400 i
0.2	3	0.919796	-0.4161530 i	1.064730	-0.4161860 i	1.21006	-0.4159410 i	1.35427	-0.4160100 i	1.49864	-0.4159740 i
0.5	0	0.770472	-0.0535483 i	0.890189	-0.0535569 i	1.00977	-0.0535626 i	1.12927	-0.0535666 i	1.24871	-0.0535695 i
0.5	1	0.769382	-0.1606750 i	0.889241	-0.1606940 i	1.00894	-0.1607060 i	1.12852	-0.1607150 i	1.24803	-0.1607210 i
0.5	2	0.767213	-0.2678890 i	0.887352	-0.2679000 i	1.00725	-0.2679080 i	1.12702	-0.2679090 i	1.24668	-0.2679080 i
0.5	3	0.764006	-0.3752250 i	0.884536	-0.3752120 i	1.00470	-0.3752150 i	1.12474	-0.3751860 i	1.24465	-0.3751530 i
0.7	0	0.698603	-0.0499479 i	0.807188	-0.0499551 i	0.915651	-0.0499599 i	1.02403	-0.0499633 i	1.13235	-0.0499658 i
0.7	1	0.697670	-0.1498670 i	0.806374	-0.1498840 i	0.914935	-0.1498940 i	1.02339	-0.1499010 i	1.13177	-0.1499060 i
0.7	2	0.695814	-0.2498500 i	0.804739	-0.2498690 i	0.913498	-0.2498700 i	1.02211	-0.2498730 i	1.13061	-0.2498750 i
0.7	3	0.693065	-0.3499210 i	0.802259	-0.3499590 i	0.911336	-0.3499190 i	1.02017	-0.3499040 i	1.12886	-0.3498910 i
1.0	0	0.618864	-0.045429 i	0.715086	-0.0454346 i	0.811196	-0.0454385 i	0.907230	-0.0454412 i	1.00321	-0.0454431 i
1.0	1	0.618111	-0.136304 i	0.714445	-0.1363150 i	0.810626	-0.1363240 i	0.906717	-0.1363310 i	1.00275	-0.1363360 i
1.0	2	0.616586	-0.227237 i	0.713183	-0.2272190 i	0.809494	-0.2272350 i	0.905685	-0.2272450 i	1.00181	-0.2272480 i
1.0	3	0.614238	-0.318292 i	0.711364	-0.3181300 i	0.807822	-0.3181750 i	0.904120	-0.3182060 i	1.00039	-0.3181990 i
1.5	0	0.531635	-0.0399653 i	0.614316	-0.0399695 i	0.696901	-0.0399722 i	0.779418	-0.0399741 i	0.861887	-0.0399755 i
1.5	1	0.531082	-0.1199080 i	0.613832	-0.1199180 i	0.696486	-0.1199220 i	0.779043	-0.1199270 i	0.861552	-0.1199300 i
1.5	2	0.529938	-0.1998980 i	0.612808	-0.1999130 i	0.695650	-0.1998900 i	0.778279	-0.1998990 i	0.860884	-0.1998940 i
1.5	3	0.528097	-0.2800320 i	0.611085	-0.2800660 i	0.694380	-0.2798920 i	0.777082	-0.2799180 i	0.859888	-0.2798720 i
2.0	0	0.478469	-0.0364115 i	0.552891	-0.0364148 i	0.627224	-0.0364171 i	0.701496	-0.0364186 i	0.775725	-0.0364197 i
2.0	1	0.478071	-0.1092340 i	0.552536	-0.1092470 i	0.626898	-0.1092550 i	0.701208	-0.1092580 i	0.775461	-0.1092620 i
2.0	2	0.477360	-0.1820240 i	0.551870	-0.1820700 i	0.626243	-0.1821050 i	0.700635	-0.1821040 i	0.774926	-0.1821120 i
2.0	3	0.476573	-0.2546100 i	0.551019	-0.2548120 i	0.625242	-0.2549820 i	0.699793	-0.2549540 i	0.774097	-0.2549860 i

We observe that, starting from $\gamma = 0$ and for increasing values, the maximum of the effective potential is shifted to the right and it also decreases. In addition, starting from $\ell = 6$ and for increasing values of ℓ , the maximum of the potential increases (comparing different values of ℓ). It should be noted that the ModMax parameter affects the QN frequencies in a non-trivial way and we can read its effect directly from the scalar effective potential (see Eq. (37) for details). Since the ModMax parameter only modifies the charged term, we have two clearly defined extremal cases: i) when $\gamma \rightarrow 0$ we recover a charged (Reissner-Nordstrom SdS or SAdS) black hole, and ii) when $\gamma \rightarrow \infty$ we recover the pure Schwarzschild-de Sitter (SdS) or Schwarzschild-Anti-de Sitter (SAdS) black hole. According to our results (see Table (I) for details), we can ensure that:

- When the ModMax parameter γ goes from zero to positive values, the quasinormal modes decrease. To be more precise, fixing $\{n, \ell\}$, we notice that as γ increases, the QN frequencies also decrease.
- Fixing the ModMax parameter γ , we observe that as n increases, the QN frequencies decrease, regardless of the angular degree ℓ .
- The ModMax parameter γ does not alter the stability of the black solution against scalar perturbations, as confirmed by the minus sign of the imaginary part of the QN frequencies. This solution is therefore stable according to this criterion.

B. Spin one case (Maxwell field)

In this section, we will introduce electromagnetic perturbations. It is essential to point out that assuming the ModMax non-linear electrodynamics, the effective Maxwell's equations take the particular form:

$$\partial_\mu \left(\sqrt{-g} e^{-\gamma} F^{\mu\nu} \right) = 0. \quad (38)$$

Notice that the last equation produces modified Maxwell's equations only if γ is a function of the spacetime. In this case, we take γ as a constant value, which means that the Maxwell's equations are not modified. So, the electromagnetic perturbations are dictated by the standard Maxwell's equations [94] according to

$$\nabla_\nu F^{\mu\nu} = 0, \quad (39)$$

where ∇_ν denotes covariant derivative.

In light that we are considering a spherically symmetric background geometry, it is possible to expand the corresponding Maxwell potential in spherical harmonics (for further details see [94] and references therein). To study electromagnetic perturbations, it is convenient to use the well-known method of separation of variables to reduce the situation to a one-dimensional problem. More precisely, after splitting the radial and angular parts, we obtain a reduced Schrödinger-like equation with a slightly different effective potential for electromagnetic perturbations. Specifically, the potential takes the reduced form [94, 95]

$$V_{EM}(r) = f(r) \left(\frac{\ell(\ell+1)}{r^2} \right), \quad \ell \geq 1 \quad (40)$$

at this point, it becomes evident that to obtain the QNMs for a given geometry, we only need to specify the lapse function $f(r)$ and subsequently solve the well-known Regge-Wheeler equation

$$\frac{d^2\psi}{dx^2} + [\omega^2 - V_{EM}(x)]\psi = 0. \quad (41)$$

The concrete form of the effective potential for electromagnetic perturbations is given as follow:

$$V_{EM}(r) = \left(k - \frac{m}{r} + \frac{q^2 e^{-\gamma}}{r^2} - \frac{\Lambda r^2}{3} \right) \left(\frac{\ell(\ell+1)}{r^2} \right). \quad (42)$$

We show, in figures, the effective potential for electromagnetic perturbations in Figure (5), middle panel, setting the parameters $\{k, m, \Lambda, q\}$ and varying ℓ from 6 to 9 as well as the ModMax parameter γ from 0 to 2, see Eq. (42) for explicit form. We observe that, similar to the massless scalar case, in the electromagnetic case the maximum of the potential increases when the angular number ℓ increases. Similarly, the maximum is shifted to the right when ℓ increases too. Even more, for a fixed ℓ , we vary the ModMax parameter γ and we observe that increasing it the effective potential decreases. Such effect transform the effective potential from a Reissner-Nordstrom SdS or SAdS black hole to a pure Schwarzschild-de Sitter (SdS) or Schwarzschild-Anti-de Sitter (SAdS) black hole. In light of our results (see Table (II) for details), we can confirm that:

- When the ModMax parameter γ goes from zero to positive values, the quasinormal modes decrease, in other words, fixing $\{n, \ell\}$, we notice that as γ increases, the QN frequencies also decrease.
- Fixing the ModMax parameter γ , we observe that as n increases, the QN frequencies decrease, regardless of the angular degree ℓ .
- As occurs in the massless scalar case, the ModMax parameter γ does not modify the stability of the black solution against electromagnetic perturbations, as is revealed by the minus sign of the imaginary part of the QN frequencies. Thus, according to this criterion the solution is stable.

C. Spin one-half case (Dirac field)

To study Dirac perturbations (i.e., fermions) we first should remember the vierbein formalism and, subsequently, we will review and show the wave equation and the effective potential (see also [96] for more details) the tetrad (or vierbein), e_a^μ , is defined as follows

$$e_\mu^a e_\nu^b \eta_{ab} = g_{\mu\nu}, \quad (43)$$

TABLE II: QN frequencies for electromagnetic perturbations, setting $k = 1$, $m = 2$, $\Lambda = 0.1$, $q = 1$ for several different values of the ModMax parameter γ and varying ℓ . For comparison reasons, we also show the frequencies of the classical geometry, i.e., when $\gamma = 0$. As in the scalar case, when the ModMax parameter increases, the quasinormal frequencies decrease. Thus, the ModMax parameter has a screening effect on the QNMs.

γ	n	$\ell = 6$	$\ell = 7$	$\ell = 8$	$\ell = 9$	$\ell = 10$
0.0	0	1.10455 -0.060301 i	1.27611 -0.0603194 i	1.44744 -0.0603333 i	1.61866 -0.060343 i	1.78981 -0.0603497 i
0.0	1	1.10197 -0.181011 i	1.27422 -0.1809900 i	1.44569 -0.1810350 i	1.61702 -0.181066 i	1.78838 -0.1810740 i
0.0	2	1.09572 -0.302344 i	1.27085 -0.3016570 i	1.44223 -0.3018340 i	1.61346 -0.301949 i	1.78548 -0.3018760 i
0.0	3	1.08260 -0.426147 i	1.26725 -0.4218510 i	1.43715 -0.4227600 i	1.60713 -0.423353 i	1.78102 -0.4228370 i
0.2	0	0.927681 -0.0593616 i	1.07183 -0.0593734 i	1.21583 -0.0593813 i	1.35971 -0.059387 i	1.50352 -0.059391 i
0.2	1	0.926250 -0.1781360 i	1.07061 -0.1781560 i	1.21477 -0.1781690 i	1.35876 -0.178182 i	1.50266 -0.178190 i
0.2	2	0.923251 -0.2971100 i	1.06812 -0.2970590 i	1.21268 -0.2970230 i	1.35685 -0.297039 i	1.50094 -0.297038 i
0.2	3	0.918293 -0.4166210 i	1.06420 -0.4162310 i	1.20965 -0.4159570 i	1.35398 -0.416003 i	1.49839 -0.415962 i
0.5	0	0.770210 -0.0535481 i	0.889961 -0.0535568 i	1.00958 -0.0535625 i	1.12909 -0.0535666 i	1.24855 -0.0535695 i
0.5	1	0.769126 -0.1606730 i	0.889010 -0.1606940 i	1.00874 -0.1607060 i	1.12834 -0.1607140 i	1.24787 -0.1607200 i
0.5	2	0.766992 -0.2678730 i	0.887102 -0.2679050 i	1.00706 -0.2679060 i	1.12684 -0.2679080 i	1.24651 -0.2679070 i
0.5	3	0.763917 -0.3751350 i	0.884220 -0.3752460 i	1.00453 -0.3752030 i	1.12458 -0.3751780 i	1.24449 -0.3751530 i
0.7	0	0.698406 -0.0499479 i	0.807018 -0.0499551 i	0.915502 -0.0499599 i	1.02390 -0.0499633 i	1.13223 -0.0499657 i
0.7	1	0.697459 -0.1498700 i	0.806198 -0.1498850 i	0.914785 -0.1498940 i	1.02326 -0.1499010 i	1.13165 -0.1499060 i
0.7	2	0.695528 -0.2498820 i	0.804528 -0.2498810 i	0.913349 -0.2498700 i	1.02197 -0.2498720 i	1.13049 -0.2498740 i
0.7	3	0.692513 -0.3501000 i	0.801924 -0.3500290 i	0.911187 -0.3499190 i	1.02004 -0.3499010 i	1.12875 -0.3498880 i
1.0	0	0.618727 -0.045429 i	0.714968 -0.0454346 i	0.811092 -0.0454385 i	0.907137 -0.0454411 i	1.00313 -0.0454431 i
1.0	1	0.617968 -0.136305 i	0.714319 -0.1363160 i	0.810520 -0.1363250 i	0.906623 -0.1363310 i	1.00266 -0.1363350 i
1.0	2	0.616408 -0.227251 i	0.713020 -0.2272330 i	0.809377 -0.2272380 i	0.905587 -0.2272470 i	1.00173 -0.2272470 i
1.0	3	0.613935 -0.318376 i	0.711067 -0.3182110 i	0.807663 -0.3181960 i	0.904004 -0.3182130 i	1.00034 -0.3181900 i
1.5	0	0.531548 -0.0399653 i	0.614243 -0.0399694 i	0.696836 -0.0399721 i	0.779359 -0.0399741 i	0.861834 -0.0399755 i
1.5	1	0.530992 -0.1199080 i	0.613770 -0.1199160 i	0.696422 -0.1199220 i	0.778989 -0.1199260 i	0.861499 -0.1199300 i
1.5	2	0.529830 -0.1999070 i	0.612809 -0.1998890 i	0.695596 -0.1998860 i	0.778247 -0.1998920 i	0.860829 -0.1998940 i
1.5	3	0.527926 -0.2800790 i	0.611320 -0.2799260 i	0.694363 -0.2798730 i	0.777135 -0.2798770 i	0.859828 -0.2798740 i
2.0	0	0.478405 -0.0364115 i	0.552835 -0.0364149 i	0.627176 -0.0364171 i	0.701453 -0.0364186 i	0.775687 -0.0364197 i
2.0	1	0.478000 -0.1092360 i	0.552463 -0.1092500 i	0.626850 -0.1092550 i	0.701163 -0.1092590 i	0.775423 -0.1092620 i
2.0	2	0.477255 -0.1820390 i	0.551704 -0.1821070 i	0.626195 -0.1821050 i	0.700582 -0.1821070 i	0.774890 -0.1821120 i
2.0	3	0.476352 -0.2546940 i	0.550515 -0.2550200 i	0.625196 -0.2549800 i	0.699707 -0.2549710 i	0.774073 -0.2549830 i

as is usual, η_{ab} is the flat Minkowski metric tensor. Also, the vierbein encodes two different kinds of indices: i) a flat index a , and ii) a spacetime index μ , and it may be viewed as the "square root" of the metric tensor $g_{\mu\nu}$.

The Dirac matrices in a curved spacetime are given as follows

$$G^\mu \equiv e_a^\mu \gamma^a, \quad (44)$$

and they satisfy the following property

$$\{\gamma^a, \gamma^b\} = -2\eta^{ab}, \quad (45)$$

$$\{G^\mu, G^\nu\} = -2g^{\mu\nu}, \quad (46)$$

where γ^a are the Dirac matrices used in relativistic quantum mechanics (in flat spacetime).

Last but not least, let us introduce the spin connection $\omega_{ab\mu}, \Gamma_\mu$ defined as follows

$$\Gamma_\mu = -\frac{1}{8}\omega_{ab\mu}[\gamma^a, \gamma^b], \quad (47)$$

$$\omega_{ab\mu} = \eta_{ac}[e_\nu^c e_b^\lambda \Gamma_{\mu\lambda}^\nu - e_b^\lambda \partial_\mu e_\lambda^c], \quad (48)$$

where $\Gamma_{\mu\lambda}^\nu$ are the Christoffel symbols.

At this point, it becomes natural to introduce the equation responsible for describing perturbation for fermions, i.e., the Dirac equation. Let us consider a spin one-half fermion Ψ in curved spacetime, in that case, the Dirac equation takes the form

$$(iG^\mu D_\mu - m_f)\Psi = 0, \quad (49)$$

being the mass of the fermion m_f , and the covariant derivative defined as $D_\mu \equiv \partial_\mu + \Gamma_\mu$. The process is equivalent to the scalar and Maxwell case, namely, we should use the method of separation of variables, where now we use the spinor spherical harmonics [98], and two radial parts

$$r^{-1}f(r)^{-1/4}F(r), \quad (50)$$

$$r^{-1}f(r)^{-1/4}iG(r), \quad (51)$$

for the upper and lower components of the Dirac spinor Ψ , respectively. For the massless case ($m_f = 0$), the equation is reduced to be [96]

$$\frac{dF}{dx} - WF + \omega G = 0, \quad (52)$$

$$\frac{dG}{dx} + WG - \omega F = 0. \quad (53)$$

As in the previous cases, x is the tortoise coordinate and the function W takes the form [96]

$$W \equiv \frac{\xi\sqrt{f}}{r}, \quad (54)$$

where $\xi \equiv \pm(j + 1/2) = \pm 1, \pm 2, \dots$, with j being the total angular momentum, $j = \ell \pm 1/2$ [96].

To conclude this part, notice first that Eqs. (52) and (53) are two first-order differential equations for F , and G . They can be conveniently combined to obtain a wave equation for each one of the following form

$$\frac{d^2F}{dx^2} + [\omega^2 - V_+]F = 0, \quad (55)$$

$$\frac{d^2G}{dx^2} + [\omega^2 - V_-]G = 0, \quad (56)$$

where the potentials are well-known and are summarized in the following expression

$$V_\pm = W^2 \pm \frac{dW}{dx}. \quad (57)$$

According to [99], and taking advantage of the language of supersymmetry, the potential V_\pm are superpartners because they are derived from a superpotential. The natural consequence of that is that they share the same spectra. Thus, in the following, we shall work with the plus sign and the wave equation for $F(r)$.

Finally, the effective potential for Dirac perturbations, taking advantage of the tortoise coordinate and writing it down in terms of ξ is given as follows

$$V_\pm = f(r) \left(\frac{\xi^2}{r^2} \pm \frac{d}{dr} \left(\frac{\xi}{r} \sqrt{f(r)} \right) \right). \quad (58)$$

Taking the positive sign and the concrete form of lapse function we finally arrive

$$V_+ = \frac{\xi \left(1 - \frac{m}{r} + \frac{q^2 e^{-\gamma}}{r^2} - \frac{\Lambda r^2}{3} \right) \left(\left(\xi \sqrt{1 - \frac{m}{r} + \frac{q^2 e^{-\gamma}}{r^2} - \frac{\Lambda r^2}{3}} + \frac{3m}{2r} - 1 \right) - \frac{2q^2 e^{-\gamma}}{r^2} \right)}{\left(\sqrt{1 - \frac{m}{r} + \frac{q^2 e^{-\gamma}}{r^2} - \frac{\Lambda r^2}{3}} \right) r^2}. \quad (59)$$

Finally, let us mention some features which can be observed in Figure (5) right panel, after observe careful the effective potential for Dirac perturbations, setting the parameters $\{k, m, \Lambda, q\}$ and varying ξ from 6 to 9 as well as the ModMax parameter γ from 0 to 2, see Eq. (59) for explicit form. As occurs in the last two cases, the maximum of the potential increases when the number ξ increases (parameter which is directly related with ℓ). Also, the maximum is shifted to the right when ξ increases, equivalently as occur in the previous two cases. Finally, varying (increasing) the ModMax parameter γ (for a fixed ξ), it is observed that the effective potential decreases.

In light of our results (see Tables (III), (IV) and (V) for details), we can confirm that:

- As occur in the previous two cases, when the ModMax parameter γ goes from zero to positive values, the quasinormal modes decrease. To confirm, please check the tables above-mentioned, i.e., fixing $\{n, \Lambda, \xi, q\}$, we notice that as γ increases, the QN frequencies also decrease (extracted from Tables (III), (IV) and (V)).
- Fixing the ModMax parameter γ , we observe that as n increases, the QN frequencies decrease, regardless of the angular degree ξ .
- As occurs in the massless scalar case and electromagnetic case, the ModMax parameter γ does not modify the stability of the black solution against Dirac perturbations. This statement is confirmed by the minus sign of the imaginary part of the QN frequencies. Thus, according to this criterion the solution is stable, at least for the range of parameters used.

V. QUASINORMAL MODES AND LYAPUNOV EXPONENT

In this part, we are interested in exploring the QNMs in large ℓ limit called eikonal limits ($\ell \rightarrow \infty$). In Ref. [83], it has been discussed that in a static and spherically symmetric spacetime, both real and imaginary parts of QNMs are related to the characteristics of circular null geodesics, via the angular velocity and the Lyapunov exponent of the photon sphere correspond, respectively, as follows

$$\omega(\ell \gg 1) = \Omega_c \ell - i \left(n + \frac{1}{2} \right) |\lambda_L|, \quad (60)$$

here, Ω_c and λ_L are the angular velocity at the unstable null geodesic, and the Lyapunov exponent, respectively. n indicates the overtone. To obtain the radius of unstable circular orbit or photonic orbit r_{ph} , first, we investigate the null geodesics via Hamiltonian of a free photon moving in the black hole background

$$H = \frac{1}{2} g^{ij} p_i p_j = 0. \quad (61)$$

Without the loss of generosity, the trajectory in the equatorial plane will be considered where $\theta = \frac{\pi}{2}$ which leads to the following equation

$$-\frac{p_t^2}{f(r)} + f(r) p_r^2 + \frac{p_\phi^2}{r^2} = 0. \quad (62)$$

As the Hamiltonian does not depend on the t and ϕ coordinates, we define two constants of motion, $E = -p_t$ and $L = p_\phi$ as energy and angular momentum respectively. Applying the Hamiltonian formalism

$$\dot{r} = \frac{\partial H}{\partial p_r} = p_r f(r). \quad (63)$$

Using the definition of the effective potential $\dot{r}^2 = V_{eff}(r) = 0$ and the two conserved quantities $\{E, L\}$, then we can write the effective potential according to

$$V_{eff}(r) = E^2 - f(r) \frac{L^2}{r^2}. \quad (64)$$

The conditions $V_{eff}(r) = 0$ and $V'_{eff}(r) = 0$ for circular null geodesics lead, respectively, to:

$$\frac{E}{L} = \pm \frac{1}{r_1} \sqrt{f(r_1)}, \quad (65)$$

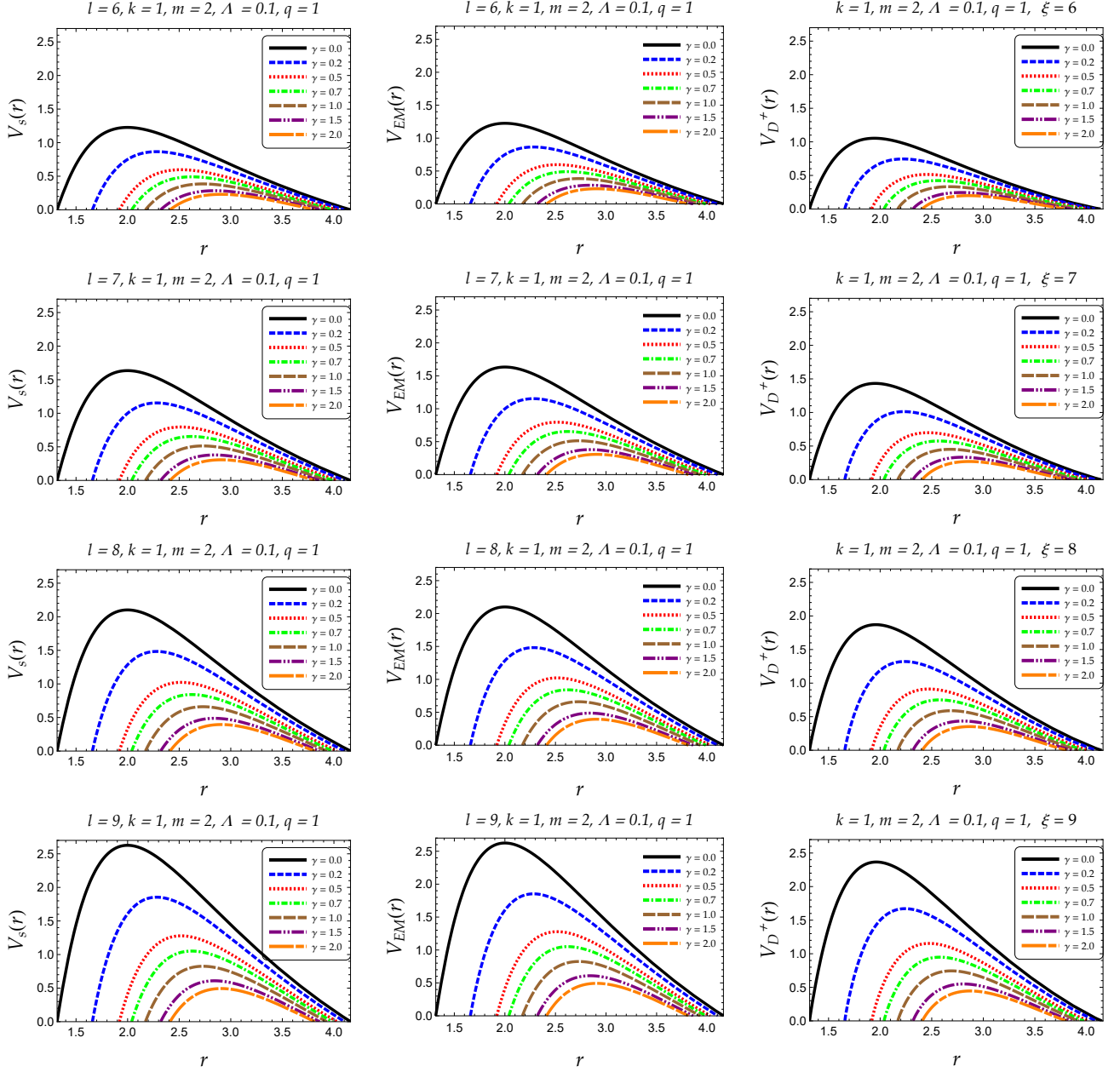


FIG. 5: Effective potential for the three types of perturbations investigated in this paper. **Left column:** scalar perturbations for different values of the MaxMod parameter γ fixing $\{\ell, k, m, \Lambda, q\}$. **Middle column:** electromagnetic perturbations for different values of the MaxMod parameter γ fixing $\{\ell, k, m, \Lambda, q\}$. **Right column:** Dirac perturbations for different values of the MaxMod parameter γ fixing $\{\xi, k, m, \Lambda, q\}$.

and

$$2f(r_1) - r_1 \left. \frac{df(r)}{dr} \right|_{r_1} = 0, \quad (66)$$

the last equation, Eq. (66), is precisely required to obtain the critical value r_1 or r_{ph} .

Thus, with the help of (66), we obtain r_{ph} as follows

$$r_{ph} = \frac{3m}{4} + \frac{\sqrt{9m^2 - 32q^2 e^{-\gamma}}}{4}. \quad (67)$$

TABLE III: QN frequencies for Dirac perturbations, setting $k = 1$, $m = 2$, $\xi = 5$ and varying the set $\{\Lambda, q, n\}$ taking the ModMax parameter $\gamma = 0.0$. This case is included for comparison reasons and it match with the published version using a different method [97].

n	Λ	$\omega(q=0.0)$	$\omega(q=0.1)$	$\omega(q=0.2)$	$\omega(q=0.3)$	$\omega(q=0.4)$	$\omega(q=0.5)$	$\omega(q=0.6)$							
0	0.00	0.960215	-0.0962564 i	0.961827	-0.0963096 i	0.966735	-0.0964676 i	0.975163	-0.0967242 i	0.987525	-0.0970661 i	1.0045	-0.0974654 i	1.02716	-0.0978635 i
0	0.01	0.916158	-0.0918083 i	0.917846	-0.0918743 i	0.9222985	-0.092071 i	0.931804	-0.0923934 i	0.944726	-0.0928303 i	0.962444	-0.0933575 i	0.986064	-0.0939224 i
0	0.02	0.869837	-0.0871387 i	0.871614	-0.0872189 i	0.877021	-0.0874586 i	0.886293	-0.0878541 i	0.899863	-0.0883962 i	0.918439	-0.0890645 i	0.943151	-0.0898121 i
0	0.03	0.820869	-0.0822089 i	0.822752	-0.0823053 i	0.828476	-0.0825937 i	0.838281	-0.0830715 i	0.852611	-0.0837319 i	0.872186	-0.0845577 i	0.898163	-0.0855079 i
0	0.04	0.768749	-0.0769683 i	0.770758	-0.0770833 i	0.776864	-0.0774278 i	0.78731	-0.0780003 i	0.802547	-0.0787957 i	0.823308	-0.0798002 i	0.850771	-0.0809784 i
0	0.05	0.712784	-0.0713475 i	0.714951	-0.0714845 i	0.721528	-0.0718954 i	0.732763	-0.0725791 i	0.749107	-0.0735323 i	0.771305	-0.0747436 i	0.800549	-0.076183 i
0	0.06	0.651986	-0.0652474 i	0.654354	-0.0654113 i	0.661534	-0.065903 i	0.67377	-0.0667218 i	0.69151	-0.0678646 i	0.715496	-0.0693218 i	0.746926	-0.0710672 i
0	0.07	0.584848	-0.0585172 i	0.587487	-0.0587157 i	0.595475	-0.0593106 i	0.609041	-0.0603003 i	0.628613	-0.0616801 i	0.654909	-0.0634409 i	0.689109	-0.0655559 i
0	0.08	0.508867	-0.0509062 i	0.511899	-0.0511512 i	0.52105	-0.0518895 i	0.536505	-0.0531081 i	0.558629	-0.054806 i	0.588067	-0.0569578 i	0.625935	-0.0595376 i
0	0.09	0.419262	-0.0419362 i	0.422939	-0.0422625 i	0.433973	-0.0432053 i	0.45242	-0.044782 i	0.478459	-0.0469606 i	0.512529	-0.049621 i	0.555579	-0.0528326 i
0	0.10	0.304224	-0.030426 i	0.309367	-0.0318253 i	0.32402	-0.0303196 i	0.348472	-0.0339389 i	0.381719	-0.0373302 i	0.423659	-0.0408849 i	0.474867	-0.0451985 i
1	0.00	0.949593	-0.290179 i	0.951226	-0.290335 i	0.956197	-0.2908 i	0.964738	-0.291554 i	0.977273	-0.292555 i	0.994493	-0.293717 i	1.01751	-0.29486 i
1	0.01	0.906891	-0.27655 i	0.908593	-0.276747 i	0.913774	-0.277332 i	0.92267	-0.27829 i	0.935712	-0.279587 i	0.953608	-0.281148 i	0.977488	-0.28281 i
1	0.02	0.861871	-0.262294 i	0.863655	-0.262534 i	0.869085	-0.263252 i	0.8784	-0.264436 i	0.892041	-0.266057 i	0.910729	-0.268053 i	0.935617	-0.270279 i
1	0.03	0.814144	-0.247293 i	0.816028	-0.247583 i	0.821756	-0.248449 i	0.831574	-0.249885 i	0.845929	-0.251867 i	0.865557	-0.254345 i	0.891632	-0.257191 i
1	0.04	0.763201	-0.231394 i	0.765206	-0.23174 i	0.7713	-0.232776 i	0.781729	-0.234499 i	0.796951	-0.236891 i	0.817709	-0.239911 i	0.845199	-0.24345 i
1	0.05	0.708342	-0.214385 i	0.710499	-0.214798 i	0.717051	-0.216034 i	0.728244	-0.218092 i	0.744537	-0.220961 i	0.766683	-0.224606 i	0.795889	-0.228935 i
1	0.06	0.648571	-0.195969 i	0.650926	-0.196462 i	0.658068	-0.197941 i	0.670241	-0.200405 i	0.6879	-0.203844 i	0.711791	-0.208229 i	0.743127	-0.21348 i
1	0.07	0.582371	-0.175689 i	0.584995	-0.176286 i	0.592935	-0.178075 i	0.606423	-0.181051 i	0.625888	-0.1852 i	0.652056	-0.190498 i	0.686114	-0.196862 i
1	0.08	0.507228	-0.152792 i	0.510239	-0.153524 i	0.519341	-0.155748 i	0.534704	-0.159403 i	0.556711	-0.164517 i	0.585994	-0.170983 i	0.623682	-0.178739 i
1	0.09	0.41834	-0.125841 i	0.42201	-0.12684 i	0.432969	-0.12963 i	0.451341	-0.134394 i	0.477297	-0.141027 i	0.511125	-0.148874 i	0.553987	-0.15855 i
1	0.10	0.303869	-0.0912867 i	0.310752	-0.0986849 i	0.320168	-0.0839339 i	0.34697	-0.0998782 i	0.3809	-0.111621 i	0.422625	-0.122188 i	0.473949	-0.13578 i
2	0.00	0.929979	-0.487634 i	0.931649	-0.487888 i	0.936736	-0.488639 i	0.94548	-0.489855 i	0.958323	-0.49146 i	0.975988	-0.493304 i	0.999629	-0.495074 i
2	0.01	0.889651	-0.464109 i	0.891378	-0.464433 i	0.896637	-0.465397 i	0.905673	-0.466974 i	0.918934	-0.469103 i	0.937156	-0.471652 i	0.96151	-0.474339 i
2	0.02	0.846942	-0.439644 i	0.84874	-0.440045 i	0.854212	-0.44124 i	0.863607	-0.443208 i	0.877381	-0.445901 i	0.896279	-0.449207 i	0.921494	-0.452877 i
2	0.03	0.801453	-0.414041 i	0.803339	-0.414525 i	0.809076	-0.415975 i	0.818917	-0.418376 i	0.833324	-0.421688 i	0.853053	-0.425822 i	0.879314	-0.430559 i
2	0.04	0.752658	-0.387036 i	0.754655	-0.387616 i	0.760728	-0.389354 i	0.771129	-0.392241 i	0.786326	-0.39625 i	0.807083	-0.401305 i	0.834627	-0.407223 i
2	0.05	0.699844	-0.358275 i	0.701985	-0.358966 i	0.708487	-0.361041 i	0.719604	-0.364491 i	0.735805	-0.369301 i	0.757856	-0.375409 i	0.786996	-0.382662 i
2	0.06	0.641995	-0.327251 i	0.644326	-0.328078 i	0.651395	-0.330557 i	0.663453	-0.334687 i	0.680959	-0.340449 i	0.704674	-0.347796 i	0.735835	-0.356596 i
2	0.07	0.577573	-0.293201 i	0.580166	-0.294201 i	0.588016	-0.297194 i	0.601354	-0.302173 i	0.620616	-0.309116 i	0.646545	-0.317994 i	0.680339	-0.328655 i
2	0.08	0.504033	-0.25486 i	0.507	-0.256072 i	0.516013	-0.259805 i	0.531188	-0.265893 i	0.552986	-0.274472 i	0.581971	-0.285283 i	0.619316	-0.298256 i
2	0.09	0.416533	-0.209823 i	0.420216	-0.211545 i	0.430973	-0.216091 i	0.449237	-0.224122 i	0.475153	-0.235443 i	0.508323	-0.248159 i	0.550856	-0.2644 i
2	0.10	0.30317	-0.152169 i	0.317694	-0.172731 i	0.303932	-0.118853 i	0.341499	-0.161073 i	0.378786	-0.185026 i	0.419961	-0.202366 i	0.47234	-0.226809 i
3	0.00	0.903578	-0.689241 i	0.905298	-0.689586 i	0.910538	-0.690606 i	0.919551	-0.692252 i	0.932804	-0.694412 i	0.951058	-0.696865 i	0.975524	-0.699153 i
3	0.01	0.866171	-0.654985 i	0.867933	-0.655434 i	0.8733	-0.656771 i	0.882528	-0.658954 i	0.89609	-0.661892 i	0.914754	-0.665393 i	0.939748	-0.669046 i
3	0.02	0.826383	-0.619585 i	0.8282	-0.620146 i	0.833735	-0.62182 i	0.843246	-0.624575 i	0.85721	-0.628339 i	0.876406	-0.632949 i	0.902075	-0.638042 i
3	0.03	0.78379	-0.582754 i	0.785681	-0.583436 i	0.791437	-0.585477 i	0.801318	-0.588855 i	0.815807	-0.593514 i	0.835689	-0.59932 i	0.86222	-0.605958 i
3	0.04	0.737839	-0.544118 i	0.739828	-0.544936 i	0.745876	-0.547388 i	0.756245	-0.551459 i	0.77142	-0.557111 i	0.792191	-0.564234 i	0.819828	-0.572563 i
3	0.05	0.687788	-0.503171 i	0.689906	-0.504146 i	0.696346	-0.507074 i	0.707363	-0.51194 i	0.723446	-0.518726 i	0.745378	-0.527337 i	0.774443	-0.537561 i
3	0.06	0.632584	-0.459197 i	0.63488	-0.460361 i	0.641851	-0.463854 i	0.653752	-0.469675 i	0.67105	-0.477797 i	0.694528	-0.488151 i	0.72546	-0.500556 i
3	0.07	0.570648	-0.411114 i	0.573199	-0.412521 i	0.580919	-0.41673 i	0.594048	-0.423735 i	0.613024	-0.433504 i	0.63863	-0.446013 i	0.672066	-0.461033 i
3	0.08	0.499385	-0.35714 i	0.502279	-0.358825 i	0.51118	-0.364092 i	0.526068	-0.372613 i	0.547596	-0.384716 i	0.576155	-0.399907 i	0.613019	-0.41815 i
3	0.09	0.413886	-0.293896 i	0.417633	-0.296394 i	0.428002	-0.302599 i	0.446176	-0.313984 i	0.47225	-0.330248 i	0.504129	-0.347491 i	0.546259	-0.370413 i
3	0.10	0.30214	-0.213074 i	0.334279	-0.253476 i	0.260522	-0.124274 i	0.32869	-0.21671 i	0.374779	-0.257461 i	0.414903	-0.281298 i	0.470328	-0.31834 i

Now, remembering that λ_L and Ω_c are, respectively, the Lyapunov exponent and the coordinate angular velocity at the unstable null geodesic (defined according to [83]), we can compute directly by means of the expressions

$$\lambda_L \equiv \sqrt{\frac{f(r_1)r_1^2}{2} \left(\frac{d^2 f(r)}{dr^2} \frac{f(r)}{r^2} \right) \Big|_{r=r_1}} = \pm r_1^2 \sqrt{\frac{g''(r_1)g(r_1)}{2}}, \quad (68)$$

$$\Omega_c \equiv \frac{\dot{\phi}(r_1)}{\dot{t}(r_1)} = \frac{\sqrt{f(r_1)}}{r_1} = \sqrt{g(r_1)}. \quad (69)$$

Also, should be mentioned that λ_L parametrize the rate of convergence or divergence of null rays in the ring's vicinity, i.e., λ_L is the decay rate of the unstable circular null geodesics. The (square of the) first parameter is then given

TABLE IV: QN frequencies for Dirac perturbations, setting $k = 1$, $m = 2$, $\xi = 5$ and varying the set $\{\Lambda, q, n\}$ taking the ModMax parameter $\gamma = 0.1$.

n	Λ	$\omega(q = 0.0)$	$\omega(q = 0.1)$	$\omega(q = 0.2)$	$\omega(q = 0.3)$	$\omega(q = 0.4)$	$\omega(q = 0.5)$	$\omega(q = 0.6)$							
0	0.00	0.960215	-0.0962564 i	0.961671	-0.0962833 i	0.966106	-0.0964475 i	0.973698	-0.0966992 i	0.984776	-0.0969827 i	0.999889	-0.0974124 i	1.01984	-0.0976272 i
0	0.01	0.916158	-0.0918083 i	0.917685	-0.0918681 i	0.922327	-0.0920461 i	0.93027	-0.0923387 i	0.941855	-0.0927369 i	0.957631	-0.0932227 i	0.978453	-0.0937583 i
0	0.02	0.869837	-0.0871387 i	0.871445	-0.0872113 i	0.876329	-0.0874283 i	0.884681	-0.0877868 i	0.89685	-0.0882797 i	0.913396	-0.0888918 i	0.935193	-0.0895898 i
0	0.03	0.820869	-0.0822089 i	0.822572	-0.0822961 i	0.827743	-0.0825571 i	0.836577	-0.08299 i	0.849431	-0.0835893 i	0.866876	-0.0843427 i	0.889806	-0.0852211 i
0	0.04	0.768749	-0.0769683 i	0.770566	-0.0770723 i	0.776083	-0.0773841 i	0.785496	-0.0779024 i	0.799169	-0.0786235 i	0.817682	-0.0795373 i	0.841947	-0.0806194 i
0	0.05	0.712784	-0.0713475 i	0.714744	-0.0714715 i	0.720687	-0.0718432 i	0.730813	-0.0724621 i	0.745487	-0.0733255 i	0.765298	-0.0744256 i	0.791166	-0.0757415 i
0	0.06	0.651986	-0.0652474 i	0.654128	-0.0653958 i	0.660617	-0.0658406 i	0.671649	-0.0665816 i	0.687587	-0.0676165 i	0.709016	-0.0689386 i	0.736862	-0.0705295 i
0	0.07	0.584848	-0.0585172 i	0.587235	-0.0586967 i	0.594456	-0.0592349 i	0.606694	-0.0601313 i	0.624294	-0.0613809 i	0.647823	-0.0629773 i	0.678187	-0.0649023 i
0	0.08	0.508867	-0.0509062 i	0.511161	-0.051113 i	0.519884	-0.0517964 i	0.533838	-0.052901 i	0.553763	-0.0544374 i	0.580164	-0.0563887 i	0.613888	-0.0587412 i
0	0.09	0.419262	-0.0419362 i	0.422586	-0.0422003 i	0.432573	-0.043089 i	0.449249	-0.0444692 i	0.472766	-0.0464741 i	0.503442	-0.0489416 i	0.541969	-0.0518527 i
0	0.10	0.304224	-0.030426 i	0.308888	-0.0317796 i	0.322427	-0.0330684 i	0.344333	-0.0333962 i	0.374452	-0.0355957 i	0.412665	-0.0405061 i	0.458857	-0.0438653 i
1	0.00	0.949593	-0.290179 i	0.951027	-0.290182 i	0.955556	-0.290741 i	0.963288	-0.291546 i	0.974464	-0.292271 i	0.989903	-0.293737 i	1.00984	-0.293718 i
1	0.01	0.906891	-0.27655 i	0.908431	-0.276728 i	0.913111	-0.277258 i	0.921122	-0.278128 i	0.932813	-0.279311 i	0.948745	-0.28075 i	0.96979	-0.282329 i
1	0.02	0.861871	-0.262294 i	0.863485	-0.262511 i	0.86839	-0.263161 i	0.87678	-0.264235 i	0.889011	-0.265709 i	0.905653	-0.267538 i	0.9276	-0.269618 i
1	0.03	0.814144	-0.247293 i	0.815848	-0.247555 i	0.821023	-0.24834 i	0.829867	-0.24964 i	0.842743	-0.25144 i	0.860231	-0.2537 i	0.88324	-0.256332 i
1	0.04	0.763201	-0.231394 i	0.765015	-0.231707 i	0.77052	-0.232645 i	0.779918	-0.234204 i	0.793575	-0.236373 i	0.812082	-0.239121 i	0.836362	-0.242732 i
1	0.05	0.708342	-0.214385 i	0.710294	-0.214758 i	0.716213	-0.215877 i	0.726301	-0.21774 i	0.740928	-0.220339 i	0.760688	-0.223649 i	0.786515	-0.227608 i
1	0.06	0.648571	-0.195969 i	0.650701	-0.196415 i	0.657155	-0.197754 i	0.668131	-0.199984 i	0.683994	-0.203098 i	0.705335	-0.207076 i	0.733089	-0.211863 i
1	0.07	0.582371	-0.175689 i	0.584744	-0.176229 i	0.591921	-0.177846 i	0.60409	-0.180544 i	0.621593	-0.184301 i	0.645003	-0.189103 i	0.675233	-0.194892 i
1	0.08	0.507228	-0.152792 i	0.509956	-0.153468 i	0.518182	-0.15547 i	0.532055	-0.158785 i	0.551869	-0.163404 i	0.578125	-0.169261 i	0.61169	-0.176345 i
1	0.09	0.41834	-0.125841 i	0.4216	-0.126543 i	0.431583	-0.129296 i	0.448101	-0.133293 i	0.471592	-0.139487 i	0.502133	-0.146931 i	0.54045	-0.155628 i
1	0.10	0.303869	-0.0912867 i	0.310273	-0.0985442 i	0.323833	-0.102539 i	0.342541	-0.0976416 i	0.371697	-0.102469 i	0.412673	-0.122977 i	0.457876	-0.131521 i
2	0.00	0.929979	-0.487634 i	0.931262	-0.487429 i	0.936082	-0.488541 i	0.944152	-0.490025 i	0.95535	-0.490895 i	0.97168	-0.493824 i	0.990699	-0.491978 i
2	0.01	0.889651	-0.464109 i	0.891213	-0.464402 i	0.895963	-0.465275 i	0.9041	-0.466707 i	0.915986	-0.468649 i	0.932201	-0.471003 i	0.953654	-0.473565 i
2	0.02	0.846942	-0.439644 i	0.848568	-0.440007 i	0.853511	-0.441089 i	0.861973	-0.442873 i	0.87432	-0.445323 i	0.891144	-0.448354 i	0.913367	-0.45179 i
2	0.03	0.801453	-0.414041 i	0.803159	-0.414479 i	0.808342	-0.415792 i	0.817206	-0.417966 i	0.830124	-0.420973 i	0.847696	-0.424746 i	0.870856	-0.429132 i
2	0.04	0.752658	-0.387036 i	0.754465	-0.387561 i	0.75995	-0.389134 i	0.769321	-0.391748 i	0.782953	-0.395382 i	0.801452	-0.399983 i	0.825766	-0.405422 i
2	0.05	0.699844	-0.358275 i	0.701781	-0.358901 i	0.707655	-0.360777 i	0.717674	-0.363901 i	0.732214	-0.368258 i	0.751883	-0.373806 i	0.777636	-0.380438 i
2	0.06	0.641995	-0.327251 i	0.644104	-0.328 i	0.650492	-0.330243 i	0.661363	-0.33398 i	0.677086	-0.339199 i	0.698263	-0.345866 i	0.725846	-0.353885 i
2	0.07	0.577573	-0.293201 i	0.579918	-0.294104 i	0.58701	-0.296808 i	0.599049	-0.301328 i	0.616366	-0.307614 i	0.639552	-0.315654 i	0.66953	-0.325348 i
2	0.08	0.504033	-0.25486 i	0.506738	-0.255998 i	0.514869	-0.259341 i	0.52858	-0.264874 i	0.548184	-0.272598 i	0.574151	-0.282369 i	0.607428	-0.294251 i
2	0.09	0.416533	-0.209823 i	0.419547	-0.210749 i	0.429635	-0.215573 i	0.445649	-0.221848 i	0.46932	-0.232659 i	0.499641	-0.245178 i	0.537491	-0.259577 i
2	0.10	0.30317	-0.152169 i	0.31721	-0.172486 i	0.330974	-0.179487 i	0.335725	-0.155595 i	0.360794	-0.158399 i	0.414552	-0.208882 i	0.455814	-0.218998 i
3	0.00	0.903578	-0.689241 i	0.904441	-0.688644 i	0.90986	-0.69047 i	0.918574	-0.692761 i	0.9295	-0.693482 i	0.94761	-0.698322 i	0.96362	-0.692986 i
3	0.01	0.866171	-0.654985 i	0.867764	-0.655392 i	0.872612	-0.656603 i	0.880921	-0.658585 i	0.893073	-0.661267 i	0.909676	-0.664504 i	0.931681	-0.668 i
3	0.02	0.826383	-0.619585 i	0.828027	-0.620092 i	0.833026	-0.621608 i	0.841591	-0.624107 i	0.854105	-0.627532 i	0.871185	-0.631761 i	0.893794	-0.636537 i
3	0.03	0.78379	-0.582754 i	0.7855	-0.583371 i	0.790699	-0.585219 i	0.799599	-0.588279 i	0.812587	-0.592509 i	0.830285	-0.597811 i	0.853667	-0.603961 i
3	0.04	0.737839	-0.544118 i	0.739638	-0.544858 i	0.745101	-0.547077 i	0.754442	-0.550764 i	0.76805	-0.555888 i	0.786552	-0.562371 i	0.810929	-0.570029 i
3	0.05	0.687788	-0.503171 i	0.689704	-0.504054 i	0.695521	-0.506701 i	0.70545	-0.511108 i	0.719878	-0.517253 i	0.739433	-0.525078 i	0.765098	-0.534427 i
3	0.06	0.632584	-0.459197 i	0.634662	-0.460251 i	0.64096	-0.463412 i	0.651688	-0.468679 i	0.667222	-0.476036 i	0.688179	-0.485433 i	0.715534	-0.496734 i
3	0.07	0.570648	-0.411114 i	0.572953	-0.412382 i	0.579924	-0.416182 i	0.591785	-0.422551 i	0.608841	-0.431394 i	0.631717	-0.442714 i	0.661347	-0.456362 i
3	0.08	0.499385	-0.35714 i	0.502066	-0.358752 i	0.510059	-0.363443 i	0.52353	-0.371202 i	0.542836	-0.38206 i	0.568375	-0.39576 i	0.601277	-0.412518 i
3	0.09	0.413886	-0.293896 i	0.416327	-0.294817 i	0.426769	-0.301934 i	0.441703	-0.310121 i	0.466046	-0.326013 i	0.496128	-0.343719 i	0.53319	-0.363733 i
3	0.10	0.30214	-0.213074 i	0.333779	-0.253119 i	0.348112	-0.263422 i	0.31933	-0.205957 i	0.333515	-0.200038 i	0.42048	-0.298349 i	0.452546	-0.306284 i

according to

$$\begin{aligned}
\lambda_L^2 &= \frac{\sqrt{9m^2 - 32q^2 e^{-\gamma}}}{16q^2 e^{-\gamma}} \left(\frac{9m^3}{32q^6 e^{-3\gamma}} \left(\frac{9m^2}{8} + 7q^2 e^{-\gamma} \right) + \frac{m}{q^2 e^{-\gamma}} \left(\frac{11}{4} + \Lambda q^2 e^{-\gamma} \right) \right) \\
&+ \frac{243m^4}{512q^8 e^{-4\gamma}} \left(q^2 e^{-\gamma} - \frac{m^2}{8} \right) - \frac{3\Lambda m^2}{16q^4 e^{-2\gamma}} \left(\frac{23}{4} + \Lambda q^2 e^{-\gamma} \right) + \frac{8}{16q^2 e^{-\gamma}} - \frac{2\Lambda}{3}, \tag{70}
\end{aligned}$$

and the second parameter is computed to be

$$\Omega_c = \frac{\sqrt{\frac{m\sqrt{9m^2 - 32q^2 e^{-\gamma}}}{2q^2 e^{-\gamma}} (1 - 4\Lambda q^2 e^{-\gamma}) - \frac{3m^2}{2q^2 e^{-\gamma}} (1 + 4\Lambda q^2 e^{-\gamma}) + \frac{32\Lambda q^2 e^{-\gamma}}{3} + 8}}{\sqrt{9m^2 - 32q^2 e^{-\gamma} + 3m}}. \tag{71}$$

Finally, let us mention that the last two expressions recover the standard results when we demand $\gamma \rightarrow 0$, and also contains the neutral case, recovered when $q \rightarrow 0$, as it should be.

TABLE V: QN frequencies for Dirac perturbations, setting $k = 1$, $m = 2$, $\xi = 5$ and varying the set $\{\Lambda, q, n\}$ taking the ModMax parameter $\gamma = 0.2$.

n	Λ	$\omega(q = 0.0)$	$\omega(q = 0.1)$	$\omega(q = 0.2)$	$\omega(q = 0.3)$	$\omega(q = 0.4)$	$\omega(q = 0.5)$	$\omega(q = 0.6)$							
0	0.00	0.960215	-0.0962564 i	0.961534	-0.0963004 i	0.965538	-0.0964247 i	0.972377	-0.0966365 i	0.982315	-0.0968823 i	0.995791	-0.0972709 i	1.01344	-0.0976058 i
0	0.01	0.916158	-0.0918083 i	0.917539	-0.0918624 i	0.921733	-0.0920236 i	0.92889	-0.092289 i	0.939287	-0.0926516 i	0.953358	-0.0930978 i	0.97177	-0.0936 i
0	0.02	0.869837	-0.0871387 i	0.871291	-0.0872044 i	0.875704	-0.0874008 i	0.883231	-0.0877257 i	0.894153	-0.0881735 i	0.908917	-0.0887329 i	0.928202	-0.0893798 i
0	0.03	0.820869	-0.0822089 i	0.822409	-0.0822878 i	0.827082	-0.0825241 i	0.835044	-0.0829161 i	0.846585	-0.0834598 i	0.862157	-0.0841459 i	0.882458	-0.084954 i
0	0.04	0.768749	-0.0769683 i	0.770393	-0.0770624 i	0.775377	-0.0773446 i	0.783864	-0.0778138 i	0.796143	-0.0784673 i	0.812679	-0.0792977 i	0.834179	-0.0802878 i
0	0.05	0.712784	-0.0713475 i	0.714557	-0.0714597 i	0.719928	-0.071796 i	0.729058	-0.0723562 i	0.742244	-0.0731382 i	0.759951	-0.0741363 i	0.782897	-0.0753362 i
0	0.06	0.651986	-0.0652474 i	0.653923	-0.0653816 i	0.659788	-0.0657843 i	0.669739	-0.0664548 i	0.684069	-0.0673917 i	0.703242	-0.0685904 i	0.727976	-0.070038 i
0	0.07	0.584848	-0.0585172 i	0.587008	-0.0586798 i	0.593535	-0.0591672 i	0.604579	-0.0599775 i	0.620417	-0.0611096 i	0.641497	-0.0625569 i	0.668521	-0.064307 i
0	0.08	0.508867	-0.0509062 i	0.511349	-0.051109 i	0.51883	-0.0517083 i	0.531433	-0.0527154 i	0.549387	-0.0541002 i	0.573091	-0.0558777 i	0.603192	-0.0580113 i
0	0.09	0.419262	-0.0419362 i	0.422279	-0.042273 i	0.431308	-0.04301 i	0.446393	-0.0442888 i	0.467633	-0.0460763 i	0.495268	-0.0482607 i	0.529821	-0.0509556 i
0	0.10	0.304224	-0.030426 i	0.308966	-0.0363733 i	0.320123	-0.0264265 i	0.340761	-0.0347901 i	0.368067	-0.0362689 i	0.402569	-0.038795 i	0.44442	-0.0425248 i
1	0.00	0.949593	-0.290179 i	0.95093	-0.29031 i	0.954976	-0.290656 i	0.961906	-0.291278 i	0.971905	-0.291854 i	0.985657	-0.293152 i	1.0035	-0.293991 i
1	0.01	0.906891	-0.27655 i	0.908284	-0.276711 i	0.912512	-0.277191 i	0.91973	-0.27798 i	0.930221	-0.279057 i	0.944428	-0.28038 i	0.963034	-0.281863 i
1	0.02	0.861871	-0.262294 i	0.863331	-0.262491 i	0.867762	-0.263079 i	0.875323	-0.264052 i	0.8863	-0.265392 i	0.901147	-0.267063 i	0.920559	-0.268993 i
1	0.03	0.814144	-0.247293 i	0.815686	-0.24753 i	0.820361	-0.24824 i	0.828332	-0.249418 i	0.839891	-0.251051 i	0.855499	-0.25311 i	0.875864	-0.255532 i
1	0.04	0.763201	-0.231394 i	0.764842	-0.231677 i	0.769816	-0.232526 i	0.778287	-0.233938 i	0.790552	-0.235903 i	0.807079	-0.238401 i	0.828587	-0.241376 i
1	0.05	0.708342	-0.214385 i	0.710107	-0.214723 i	0.715456	-0.215735 i	0.724552	-0.217421 i	0.737694	-0.219775 i	0.755353	-0.222779 i	0.778255	-0.226389 i
1	0.06	0.648571	-0.195969 i	0.650498	-0.196372 i	0.656331	-0.197584 i	0.666231	-0.199602 i	0.680492	-0.202421 i	0.699583	-0.206029 i	0.724229	-0.210384 i
1	0.07	0.582371	-0.175689 i	0.584518	-0.176178 i	0.591007	-0.177645 i	0.601986	-0.18008 i	0.617736	-0.183485 i	0.638708	-0.187838 i	0.665608	-0.193103 i
1	0.08	0.507228	-0.152792 i	0.509697	-0.153406 i	0.517127	-0.155192 i	0.529669	-0.158239 i	0.547509	-0.162375 i	0.571094	-0.167731 i	0.601038	-0.174138 i
1	0.09	0.41834	-0.125841 i	0.421481	-0.127111 i	0.43038	-0.129164 i	0.445372	-0.132967 i	0.466529	-0.138378 i	0.493932	-0.144756 i	0.528367	-0.152948 i
1	0.10	0.303869	-0.0912867 i	0.320049	-0.126953 i	0.311094	-0.0585326 i	0.342185	-0.107868 i	0.367555	-0.10893 i	0.401061	-0.114813 i	0.443177	-0.12686 i
2	0.00	0.929979	-0.487634 i	0.931374	-0.487896 i	0.935443	-0.488358 i	0.942541	-0.489371 i	0.952352	-0.489721 i	0.966921	-0.492412 i	0.984936	-0.493353 i
2	0.01	0.889651	-0.464109 i	0.891064	-0.464374 i	0.895355	-0.465165 i	0.902686	-0.466464 i	0.913349	-0.468234 i	0.927806	-0.470399 i	0.946763	-0.472813 i
2	0.02	0.846942	-0.439644 i	0.848413	-0.439972 i	0.852879	-0.440952 i	0.860503	-0.44257 i	0.871582	-0.444796 i	0.886586	-0.447569 i	0.906232	-0.45076 i
2	0.03	0.801453	-0.414041 i	0.802996	-0.414438 i	0.807679	-0.415625 i	0.815667	-0.417595 i	0.827262	-0.420324 i	0.842938	-0.423762 i	0.863426	-0.4278 i
2	0.04	0.752658	-0.387036 i	0.754292	-0.387512 i	0.759249	-0.388935 i	0.767695	-0.391301 i	0.779935	-0.394595 i	0.796449	-0.398777 i	0.817975	-0.403756 i
2	0.05	0.699844	-0.358275 i	0.701596	-0.358841 i	0.706904	-0.360539 i	0.715937	-0.363366 i	0.728998	-0.367313 i	0.74657	-0.372347 i	0.769395	-0.378396 i
2	0.06	0.641995	-0.327251 i	0.643902	-0.327927 i	0.649676	-0.329959 i	0.65948	-0.333339 i	0.673612	-0.338064 i	0.692552	-0.344109 i	0.717035	-0.351406 i
2	0.07	0.577573	-0.293201 i	0.579696	-0.294022 i	0.586111	-0.296476 i	0.596964	-0.300547 i	0.612553	-0.306256 i	0.633313	-0.313533 i	0.65998	-0.322348 i
2	0.08	0.504033	-0.25486 i	0.506488	-0.255905 i	0.513786	-0.258823 i	0.526248	-0.263991 i	0.543823	-0.270815 i	0.567227	-0.279871 i	0.596836	-0.290508 i
2	0.09	0.416533	-0.209823 i	0.419721	-0.211577 i	0.428448	-0.215148 i	0.443237	-0.221455 i	0.464315	-0.230654 i	0.491132	-0.241016 i	0.525597	-0.255232 i
2	0.10	0.30317	-0.152169 i	0.316763	-0.172249 i	0.285112	+0.0692093 i	0.349571	-0.188813 i	0.366687	-0.181886 i	0.394612	-0.183928 i	0.438893	-0.207583 i
3	0.00	0.903578	-0.689241 i	0.905072	-0.689637 i	0.9091	-0.69015 i	0.916423	-0.691528 i	0.925507	-0.691249 i	0.941686	-0.695683 i	0.959551	-0.696324 i
3	0.01	0.866171	-0.654985 i	0.867612	-0.655353 i	0.871991	-0.65645 i	0.879477	-0.658249 i	0.890376	-0.660694 i	0.905173	-0.663676 i	0.924608	-0.666978 i
3	0.02	0.826383	-0.619585 i	0.82787	-0.620044 i	0.832386	-0.621416 i	0.840102	-0.623681 i	0.851328	-0.626795 i	0.866555	-0.630666 i	0.886531	-0.635108 i
3	0.03	0.78379	-0.582754 i	0.785337	-0.583312 i	0.790034	-0.584985 i	0.798053	-0.587757 i	0.809707	-0.591596 i	0.82549	-0.596428 i	0.846161	-0.602095 i
3	0.04	0.737839	-0.544118 i	0.739467	-0.544788 i	0.744402	-0.546796 i	0.752821	-0.550133 i	0.765035	-0.554778 i	0.781544	-0.560673 i	0.80311	-0.567685 i
3	0.05	0.687788	-0.503171 i	0.689521	-0.50397 i	0.694776	-0.506364 i	0.703727	-0.510353 i	0.716685	-0.515921 i	0.734146	-0.523021 i	0.756877	-0.53155 i
3	0.06	0.632584	-0.459197 i	0.634462	-0.460148 i	0.640157	-0.463013 i	0.649828	-0.467776 i	0.663786	-0.474435 i	0.682522	-0.482957 i	0.706786	-0.493239 i
3	0.07	0.570648	-0.411114 i	0.572739	-0.41227 i	0.579052	-0.415725 i	0.589722	-0.421445 i	0.605091	-0.429489 i	0.625554	-0.439725 i	0.651899	-0.452137 i
3	0.08	0.499385	-0.35714 i	0.501834	-0.358631 i	0.508899	-0.36265 i	0.521301	-0.37001 i	0.538431	-0.379475 i	0.561635	-0.39231 i	0.590732	-0.40719 i
3	0.09	0.413886	-0.293896 i	0.417469	-0.296666 i	0.425721	-0.301426 i	0.440146	-0.31016 i	0.461222	-0.323279 i	0.486813	-0.337201 i	0.521631	-0.357762 i
3	0.10	0.30214	-0.213074 i	0.333302	-0.252763 i	0.368464	+0.290771 i	0.367417	-0.277134 i	0.365654	-0.255162 i	0.38039	-0.247944 i	0.430334	-0.286034 i

VI. EMISSION RATE

Quantum fluctuations inside the black holes, create and annihilate a large number of particles near the horizon. Particles with positive energy can escape from black hole via tunneling effect. This phenomenon causes gradual black hole evaporation over a period of time known as Hawking radiation. For a distant observer, black hole shadow corresponds to the high energy absorption cross section which is shown that it is around a limiting constant value [100]

$$\sigma_{lim} \approx \pi R_{sh}^2 \quad (72)$$

where R_{sh} is the shadow radius. Then, the expression for the rate of energy emission can be written as [100–104]

$$\frac{d^2 E}{d\omega dt} = \frac{2\pi^2 \sigma_{lim}}{e^{\frac{\omega}{T_H}} - 1} \omega^3 \quad (73)$$

To obtain the shadow radius, The radius of shadow detected by an observer at spatial infinity is related to the

critical orbit and the observer's position r_O as [105]

$$R_{sh} = r_c \sqrt{\frac{f(r_O)}{f(r_c)}} = \frac{\left(\sqrt{9m^2 - 32q^2 e^{-\gamma}} + 3m\right) \sqrt{1 - \frac{m}{r_O} + \frac{q^2 e^{-\gamma}}{r_O^2} - \frac{\Lambda r_O^2}{3}}}{\sqrt{\frac{m\sqrt{9m^2 - 32q^2 e^{-\gamma}}}{2q^2 e^{-\gamma}} (1 - 4\Lambda q^2 e^{-\gamma}) - \frac{3m^2}{2q^2 e^{-\gamma}} (1 + 4\Lambda q^2 e^{-\gamma}) + \frac{8}{3} (3 + 4\Lambda q^2 e^{-\gamma})}}. \quad (74)$$

By substituting the Hawking temperature from Eq. (24) and R_{sh} from Eq. (74) in Eq. (73), the energy emission rate can be calculated. The behavior of energy emission rate with respect to ω for fixed values of cosmological constant and different values of ModMax parameter for $m = 1$, $q = 0.3$ and $r_O = 3$ are represented in Fig. 6

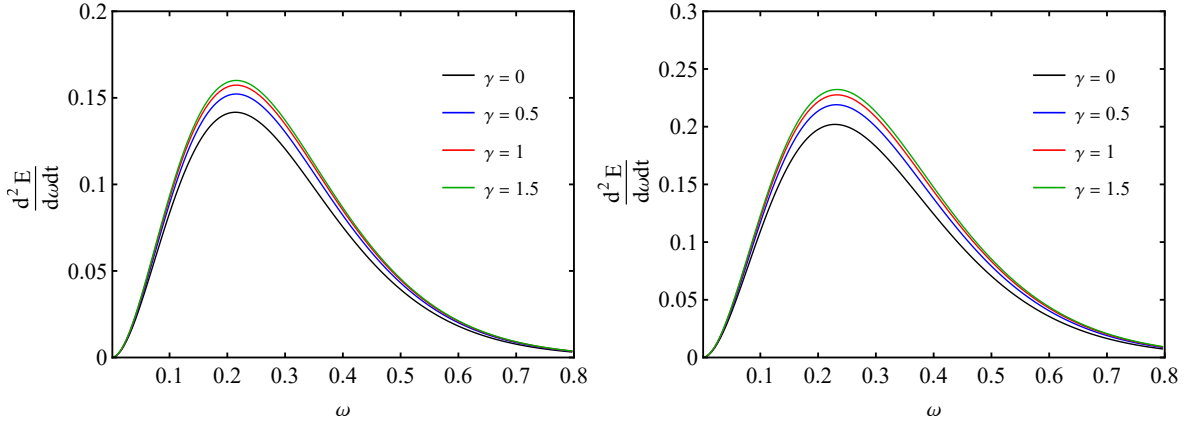


FIG. 6: The emission rate versus frequency for $k = 1$, $m = 1$, $q = 0.3$ and different values of the γ . Left panel for dS case ($\Lambda = +0.003$). Right panel for AdS case ($\Lambda = -0.003$).

In Fig. 6, left panel shows the dS case with positive cosmological constant $\Lambda = 0.003$. It can be noticed that when the ModMax parameter becomes higher the peak of energy emission rate goes up and the maximum energy emission rate occurs at bigger frequency. The right panel, demonstrates the AdS case for $\Lambda = -0.003$. The variation of emission rate versus frequency for different values of γ has the same behavior as dS case. The bigger values of γ leads to higher emission rate and shift the maximum of plots to higher frequency. This indicates that the higher ModMax parameter corresponds to the faster evaporation process in black hole in both dS and AdS spacetime.

The energy emission rate against the frequency are shown for $m = 1$, $q = 0.3$, $\gamma = 1$ and different values of the cosmological constant in Fig. 7. The left panel shows that the rate of emission energy is become smaller for higher values of Λ in dS spacetime and it means that increasing the cosmological constant in this spacetime yields to slower evaporation process and a longer lifetime for the black hole. Moreover, the peak of the emission rate decreases with increasing Λ and shifts to the lower frequency. In the right panel, the emission rate versus frequency is described for AdS spacetime and various values of Λ . When the absolute value of Λ increases the peak of emission rate increases as well and it shifts to higher right, which means that the maximum emission rate happens in higher frequency. These results imply that the the evaporation of the black hole is high for smaller absolute values of Λ in AdS spacetime.

VII. CONCLUSIONS

To summarize our work, in the present paper we have studied several aspects of topological (A)dS black holes combined with ModMax non-linear electrodynamics. In particular, we have investigated the quasinormal spectra for massless scalar, electromagnetic as well as Dirac perturbations in four-dimensional non-linearly charged dS black holes. We start by revisiting the basic idea and relevance of the QNMs. Thus, we discuss the method used to compute the quasinormal frequencies we present the effective potential and some figures. The QN frequencies were obtained taking

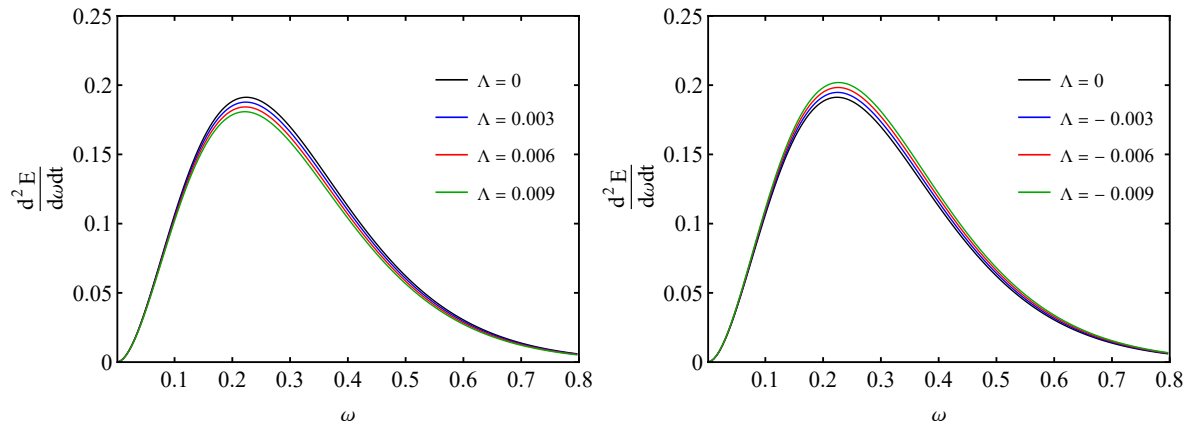


FIG. 7: The emission rate versus frequency for $k = 1$, $m = 1$, $q = 0.3$, $\gamma = 1$ and different values of the Λ . Left panel for dS case ($\Lambda > 0$). Right panel for AdS case ($\Lambda < 0$).

advantage WKB method of 6th order. We present our results in tables, where we show the impact on the spectrum of the overtone number n , the angular degree ℓ (or equivalently the parameter ξ) and the ModMax parameter γ . At least for the numerical values used, all the modes are found to be stable against the three types of perturbations. Thus, from tables, we can read that:

- When the ModMax parameter γ goes from zero to positive values, the quasinormal modes decrease, in other words, fixing $\{n, \ell(\text{or } \xi)\}$, we notice that as γ increases, the QN frequencies also decrease.
- Fixing the ModMax parameter γ , we observe that as n increases, the QN frequencies decrease, regardless of the parameter $\ell(\text{or } \xi)$.
- In all the cases, the ModMax parameter γ does not modify the stability of the black solution against scalar/electromagnetic/Dirac perturbations, as is revealed by the minus sign of the imaginary part of the QN frequencies. Thus, according to this criterion the solution is stable.

Moreover, circular null geodesics were studied to investigate the QNMs in the eikonal limit. By obtaining the angular velocity as the real part and the Lyapunov exponent as the imaginary component of QNMs, an analytical expression for QNMs has been derived. Finally, the impact of the cosmological constant and ModMax parameter on the energy emission rate has been investigated. It was shown that the rate of energy emission is higher for the higher value of γ for both dS and AdS spacetime, which means that a higher ModMax parameter makes the black hole's lifetime shorter. For a fixed value of the ModMax parameter, in dS spacetime, when the cosmological constant increased the peak of the emission rate decreased, and for AdS spacetime, high absolute values of Λ led to a higher peak in the emission rate.

Acknowledgments

BEP and NH would like to thank University of Mazandaran. A. R. acknowledges financial support from Conselleria d'Educació, Cultura, Universitats i Ocupació de la Generalitat Valenciana through Prometeo Project CIPROM/2022/13. A. R. is funded by the María Zambrano contract ZAMBRANO 21-25 (Spain) (with funding from NextGenerationEU).

-
- [1] M. Born, and L. Infeld, Proc. R. Soc. Lond. 144 (1934) 425.
[2] E. S. Fradkin, and A. A. Tseylin, Phys. Lett. B 163 (1985) 123.
[3] G. W. Gibbons, and C. A. R. Herdeiro, Class. Quantum Grav. 18 (2001) 1677.
[4] G. W. Gibbons, and D. A. Rasheed, Nucl. Phys. B 454 (1995) 185.

- [5] I. Bandos, K. Lechner, D. Sorokin, and P. K. Townsend, *Phys. Rev. D* 102 (2020) 121703.
- [6] B. P. Kosyakov, *Phys. Lett. B* 810 (2020) 135840.
- [7] D. Flores-Alfonso, B. A. Gonzalez-Morales, R. Linares, and M. Maceda, *Phys. Lett. B* 812 (2021) 136011.
- [8] I. Bandos, K. Lechner, D. Sorokin, and P. K. Townsend, *JHEP* 03 (2021) 022; *JHEP* 10 (2021) 031.
- [9] S. I. Kruglov, *Phys. Lett. B* 822 (2021) 136633.
- [10] S. M. Kuzenko, and E. S. N. Raptakis, *Phys. Rev. D* 104 (2021) 125003.
- [11] Z. Avetisyan, O. Evnin, and K. Mkrtchyan, *Phys. Rev. Lett.* 127 (2021) 271601.
- [12] P. A. Cano, and A. Murcia, *JHEP* 08 (2021) 042.
- [13] A. Ballon Bordo, D. Kubiznak, and T. Perche, *Phys. Lett. B* 817 (2021) 136312.
- [14] A. Bokulic, I. Smolic, and T. Juric, *Phys. Rev. D* 103 (2021) 124059.
- [15] H. Babaei-Aghbolagh, et al., *Phys. Lett. B* 829 (2022) 137079.
- [16] H. Babaei-Aghbolagh, et al., *JHEP* 12 (2022) 147.
- [17] C. A. Escobar, and R. Linares, *Phys. Rev. D* 106 (2022) 036027.
- [18] J. Barrientos, A. Cisterna, D. Kubiznak, and J. Oliva, *Phys. Lett. B* 834 (2022) 137447.
- [19] R. C. Pantig, L. Mastrototaro, G. Lambiase, and A. Ovgun, *Eur. Phys. J. C* 82 (2022) 1155.
- [20] A. Bokulic, T. Juric, and I. Smolic, *Phys. Rev. D* 106 (2022) 064020.
- [21] K. Lechner, P. Marchetti, A. Sainaghi, and D. P. Sorokin, *Phys. Rev. D* 106 (2022) 016009.
- [22] M. Ortaggio, *Eur. Phys. J. C* 82 (2022) 1056.
- [23] H. Nastase, *Phys. Rev. D* 105 (2022) 105024.
- [24] A. Ali, and K. Saifullah, *Annals Phys.* 437 (2022) 168726.
- [25] J. B. Jimenez, D. Bettoni, and P. Brax, *JHEP* 02 (2023) 009.
- [26] C. Ferko, and A. Gupta, *Phys. Rev. D* 108 (2023) 046013.
- [27] S. M. Kuzenko, and I. N. McArthur, *JHEP* 05 (2023) 127.
- [28] H. Rathi, and D. Roychowdhury, *JHEP* 07 (2023) 026.
- [29] H. M. Siahaan, *Int. J. Mod. Phys. D* 32 (2023) 2350099.
- [30] B. Eslam Panah, *Prog. Theor. Exp. Phys.* 2024 (2024) 023E01.
- [31] B. Eslam Panah, B. Hazarika, and P. Phukon, *Prog. Theor. Exp. Phys.* 2024 (2024) 083E02.
- [32] H. M. Siahaan, *Commun. Theor. Phys.* 76 (2024) 065402.
- [33] B. Eslam Panah, *Contrib. Sci. Tech Eng.* 1(3) (2024) 25.
- [34] J. D. Bekenstein, *Phys. Rev. D* 7 (1973) 2333; S. W. Hawking, *Nature.* 248 (1974) 3.
- [35] H. Kleinert, *Phys. Rev. D* 60 (1999) 085001.
- [36] H. B. Callen, John Wiley-Sons, Inc., New York, 1985.
- [37] A. L. Greer, *Science.* 267 (1995) 1947.
- [38] D. C. Zou, Y. Liu, and R. Yue, *Eur. Phys. J. C* 77 (2017) 365.
- [39] D. Layzer, Oxford Univ. Press, 1991.
- [40] E. Witten, *Adv. Theor. Math. Phys.* 2 (1998) 505.
- [41] D. Kubiznak, R. B. Mann, and M. Teo, *Class. Quantum Grav.* 34 (2017) 6 063001.
- [42] D. Kastor, S. Ray, and J. Traschen, *Class. Quantum Grav.* 26 (2009) 195011.
- [43] T. Regge, and J. A. Wheeler, *Phys. Rev.* 108 (1957) 1063.
- [44] F. J. Zerilli, *Phys. Rev. Lett.* 24 (1970) 737.
- [45] F. J. Zerilli, *Phys. Rev. D* 2 (1970) 2141.
- [46] F. J. Zerilli, *Phys. Rev. D* 9 (1974) 860.
- [47] V. Moncrief, *Phys. Rev. D* 12 (1975) 1526.
- [48] S. A. Teukolsky, *Phys. Rev. Lett.* 29 (1972) 1114.
- [49] S. Alfaro, et al., *Phys. Rev. D* 109 (2024) 104009.
- [50] R. Bécar, P. A. González, and Y. Vásquez, *Eur. Phys. J. C* 83 (2023) 75.
- [51] P. A. González, E. Papantonopoulos, Á. Rincón, and Y. Vásquez, *Phys. Rev. D* 106 (2022) 024050.
- [52] S. Fernando, P. A. González, and Y. Vásquez, *Eur. Phys. J. C* 82 (2022) 600.
- [53] N. Bretón, T. Clark, and S. Fernando, *Int. J. Mod. Phys. D* 26 (2017) 1750112.
- [54] S. Fernando, *Gen. Rel. Grav.* 48 (2016) 24.
- [55] Á. Rincón, A. Övgün, and R. C. Pantig, *Phys. Dark Univ.* 46 (2024) 101623.
- [56] D. J. Gogoi, A. Övgün, and D. Demir, *Phys. Dark Univ.* 42 (2023) 101314.
- [57] A. Baruah, A. Övgün, and A. Deshamukhya, *Annals Phys.* 455 (2023) 169393.
- [58] D. J. Gogoi, A. Övgün, and M. Koussour, *Eur. Phys. J. C* 83 (2023) 700.
- [59] A. Övgün, R. C. Pantig, and Á. Rincón, *Eur. Phys. J. Plus.* 138 (2023) 192.
- [60] R. C. Pantig, L. Mastrototaro, G. Lambiase, and A. Övgün, *Eur. Phys. J. C* 82 (2022) 1155.
- [61] R. D. B. Fontana, and A. Rincon, [arXiv:2404.09936 [gr-qc]].
- [62] R. Dal Bosco Fontana, *Class. Quant. Grav.* 41 (2024) 145010.
- [63] G. Panotopoulos, and Á. Rincón, *Int. J. Mod. Phys. D* 27 (2017) 1850034.
- [64] Á. Rincón, and G. Panotopoulos, *Phys. Rev. D* 97 (2018) 024027.
- [65] K. Destounis, G. Panotopoulos, and Á. Rincón, *Eur. Phys. J. C* 78 (2018) 139.
- [66] Á. Rincón, and G. Panotopoulos, *Eur. Phys. J. C* 78 (2018) 858.

- [67] G. Panotopoulos, and Á. Rincón, *Eur. Phys. J. Plus.* 134 (2019) 300.
- [68] G. Panotopoulos, and Á. Rincón, *Eur. Phys. J. Plus.* 135 (2020) 33.
- [69] Á. Rincón, and G. Panotopoulos, *Phys. Dark Univ.* 30 (2020) 100639.
- [70] Á. Rincón, and V. Santos, *Eur. Phys. J. C* 80 (2020) 910.
- [71] G. Panotopoulos, and Á. Rincón, *Phys. Dark Univ.* 31 (2021) 100743.
- [72] L. Balart, S. Belmar-Herrera, G. Panotopoulos, and Á. Rincón, *Annals Phys.* 454 (2023) 169329.
- [73] A. Rincon, and G. Gómez, *Phys. Dark Univ.* 46 (2024) 101576.
- [74] L. Balart, G. Panotopoulos, and Á. Rincón, *Fortsch. Phys.* 71 (2023) 2300075.
- [75] R. A. Konoplya, *Phys. Rev. D* 68 (2003) 024018.
- [76] R. A. Konoplya, A. Zhidenko, and A. F. Zinhailo, *Class. Quant. Grav.* 36 (2019) 155002.
- [77] V. Cardoso, R. Konoplya and J. P. S. Lemos, *Phys. Rev. D* 68 (2003) 044024.
- [78] K. D. Kokkotas, and B. G. Schmidt, *Living Rev. Rel.* 2 (1999) 2.
- [79] E. Berti, V. Cardoso, and A. O. Starinets, *Class. Quant. Grav.* 26 (2009) 163001.
- [80] R. A. Konoplya, and A. Zhidenko, *Rev. Mod. Phys.* 83 (2011) 793.
- [81] S. Chandrasekhar, "The mathematical theory of black holes, Clarendon Press, 1998.
- [82] B. Mashhoon, *Phys. Rev. D* 31 (1985) 290.
- [83] V. Cardoso, A. S. Miranda, E. Berti, H. Witek, and V. T. Zanchin, *Phys. Rev. D* 79 (2009) 064016.
- [84] K. Jusufi, *Phys. Rev. D* 101 (2020) 084055.
- [85] N. Breton, and L. A. Lopez, *Phys. Rev. D* 104 (2021) 024064.
- [86] S. Giri, H. Nandan, L.K. Joshi, and S. D. Maharaj, *Eur. Phys. J. Plus*, 137 (2022) 1.
- [87] M. Mondal, P., Pradhan, F. Rahaman, and I. Karar, *Mod. Phys. Lett. B* 35 (2020) 2050249.
- [88] G. Abbas, and R. H. Ali, *Eur. Phys. J. C* 83 (2023) 1.
- [89] A. Ashtekar, and A. Magnon, *Class. Quantum Grav.* 1 (1984) L39.
- [90] A. Ashtekar, and S. Das, *Class. Quantum Grav.* 17 (2000) L17.
- [91] L. C. B. Crispino, A. Higuchi, E. S. Oliveira, and J. V. Rocha, *Phys. Rev. D* 87 (2013) 104034.
- [92] P. Kanti, T. Pappas, and N. Pappas, *Phys. Rev. D* 90 (2014) 124077.
- [93] T. Pappas, P. Kanti, and N. Pappas, *Phys. Rev. D* 94 (2016) 024035.
- [94] V. Cardoso, and J. P. S. Lemos, *Phys. Rev. D* 64 (2001) 084017.
- [95] V. Cardoso, and J. P. S. Lemos, *Phys. Rev. D* 67 (2003) 084020.
- [96] K. Destounis, *Phys. Lett. B* 795 (2019) 211.
- [97] J. l. Jing, *Phys. Rev. D* 69 (2004) 084009.
- [98] F. Finster, J. Smoller, and S. T. Yau, *J. Math. Phys.* 41 (2000) 2173.
- [99] F. Cooper, A. Khare, and U. Sukhatme, *Phys. Rept.* 251 (1995) 267.
- [100] S. W. Wei, Y. X. Liu, *J. Cosmol. Astropart. Phys.* 11 (2013) 063.
- [101] U. Papnoi, F. Atamurotov, S. G. Ghosh, B. Ahmedov, *Phys. Rev. D* 90 (2014) 024073.
- [102] B. Eslam Panah, Kh. Jafarzade, and S. H. Hendi, *Nucl. Phys. B* 961 (2020) 115269.
- [103] S. H. Hendi, Kh. Jafarzade, and B. Eslam Panah, *J. Cosmol. Astropart. Phys.* 2 (2023) 022.
- [104] Y. Yang, D. Liu, A. Ovgun, G. Lambiase, and Z. W. Long, *Phys. Rev. D* 109 (2024) 024002.
- [105] V. Perlick, and O. Y. Tsupko, *Phys. Rep.* 947 (2022) 1.